

Assessing the influence of displacement rates on the failure behavior and undrained shear strength characteristics of reconstituted varve laminae prepared at different moisture contents

Deepali Anand^a, Arindam Dey^{*} and K. Ravi^b

Department of Civil Engineering, Indian Institute of Technology Guwahati, Amingaon, North Guwahati, Guwahati, Assam 781039, India

(Received November 19, 2024, Revised September 23, 2025, Accepted September 24, 2025)

Abstract. The geotechnical behavior of varved clays in cold regions remains inadequately understood despite their widespread occurrence. This study addresses this gap by investigating the behavior of homogeneous and reconstituted varved clay samples through Unconfined Compressive Strength (UCS) testing. Homogeneous samples consist of Red Soil (RS) and Black Soil (BS), while reconstituted varved clays are prepared by layering RS and BS in configurations of 2, 4, 8, and 16 layers. UCS tests are conducted at displacement rates of 1.25, 0.24, and 0.024 mm/min, hypothesized to simulate the velocity of glacial override on soils. Samples are prepared at five moisture contents ranging from 0.8 to 1.2 OMC. Results indicate that as moisture content decreases below OMC, undrained shear strength increases for all samples, accompanied by a reduction in strain, while the opposite trend is observed for samples on the wet side of OMC. For reconstituted varved clays, undrained shear strength increases as number of laminae rises from 2 to 8, but decreases in the 16-laminae sample, which suggests a threshold exists for the number of laminae beyond which strength reduces. Displacement rate significantly influences failure modes and patterns, with samples exhibiting more ductile behavior at lower displacement rates and higher moisture contents.

Keywords: displacement rate; moisture content; reconstituted varve laminae; unconfined compressive strength test; undrained shear strength

1. Introduction

Varved clays are a common type of laminated soil deposit found in glacial environments. These soils are characterized by distinct light and dark-colored bands arranged alternately and repetitively. The dark bands constitute clay-dominant laminae deposited during the winter season, while the light bands constitute silt-dominant laminae deposited during the summer season (Hang 2003, Ehlers 2022). These laminae form due to the unique interaction of the turbulence and temperature of the lake water with the density distribution of sediment particles transported by moving and melting glaciers during the summer season. As winter begins and temperatures drop below freezing point, the melting of glaciers stops, their movement slows down, and no fresh debris is added to the lake. In the still water conditions, the leftover fine particles from the summer settle on top of the coarser layer. This alternating settlement of coarse and fine particles creates a clear division, with visible light-colored and dark-colored laminae. One pair of light and dark-colored bands together

forms a couplet. When these couplets repeat year after year, the deposits are known as varves or varved clays (Lamoureux and Bradley 1996, Lindqvist and Lee 2009).

The engineering properties of the two soils that constitute the laminae in varves exhibit significantly different mechanical and infiltration responses under varying stress conditions, making these soils inherently anisotropic (Leroueil *et al.* 1990, Tankiewicz 2015, Dobak *et al.* 2018, Schneider *et al.* 2022, Tornborg *et al.* 2023, Philippe *et al.* 2023). The darker lamina contains more clay-sized particles, has a higher natural moisture content in field conditions, lower hydraulic conductivity, higher plasticity, lower strength, and exhibits greater volumetric changes under load compared to the lighter-colored lamina (Florkiewicz *et al.* 2014, Fliieger-Szymanska *et al.* 2019). Despite these contrasting properties between the two soils forming the laminae, the anisotropic behavior of varved clays is often overlooked due to the complexity of measuring various anisotropic parameters (Lacasse *et al.* 1977). This study addresses this gap by investigating the undrained shear strength and failure pattern characteristics of both homogenous and reconstituted varved clays with varying numbers of laminae using Unconfined Compressive Strength (UCS) tests.

UCS represents the load at which soil fails under axial compressive stress without lateral confinement and is influenced by factors such as soil type, displacement rate, temperature, and moisture content (Hampton and Yoder 1958). There are very few studies that have explored the variation in shear strength behavior of soils with changes in

*Corresponding author, Associate Professor

E-mail: arindamdey@iitg.ac.in

^aResearch Scholar

E-mail: a.deepali@iitg.ac.in

^bAssociate Professor

E-mail: ravi.civil@iitg.ac.in

these parameters, and even fewer studies specifically focus on varved clays or layered soil structures. Lo and Milligan (1967) conducted a comparative study on homogeneous and stratified clays and reported that the shear behavior of these two soil types differed considerably. The undrained strength of stratified clays was found to depend on the orientation of the stratification relative to the applied principal stresses. Awolaye *et al.* (1991) conducted UCS tests on clays at strain rates ranging from 0.08 mm/min to 2 mm/min and reported an increase in strength with a decrease in strain rate. Sabatini *et al.* (2002) found that even small variations in moisture content significantly affect soil strength under unconfined loading. Lydzba and Tankiewicz (2012) performed UCS tests on varved clays with bedding planes oriented at angles between 0° and 90° and reported that the resulting shear strength varied significantly, with the maximum strength being 14 times higher than the minimum. However, no clear trend was established between soil strength and bedding plane orientation. Du *et al.* (2016) conducted UCS tests on frozen silty sands by varying negative temperature, moisture content, and applied strain rate. Brittle failure and a non-linear increase in strength at low moisture content and higher strain rates as the sample temperature decreased was reported. At lower strain rates, an increase in moisture content resulted in decreased strength. Tyagi *et al.* (2019) performed UCS tests on soil at different strain rates by mixing it with various proportions of cement and reported a decrease in unconfined compressive strength with higher strain rates. Girgis (2020) carried out UCS tests on artificially frozen clay samples with temperatures ranging from -15°C to 0°C. For samples frozen at low temperatures and tested at high deformation rates, brittle failure in samples was observed with post-peak softening behavior, whereas for samples frozen at temperatures near freezing and tested at low displacement rates, a ductile nature of failure associated with strain hardening was observed. Sahlabadi *et al.* (2021) carried out UCS tests on soil by varying several parameters, one of which was moisture content. The strength was higher at moisture content corresponding to the Optimum Moisture Content (OMC) compared to 0.8 OMC and 1.2 OMC. Mousavi *et al.* (2021) conducted UCS tests on fine-grained soils by varying the moisture content and found a non-linear decrease in strength, coefficient of variation, and standard deviation with an increase in moisture content. Zarei *et al.* (2023) conducted triaxial tests under consolidated undrained conditions on soils with a significant amount of clay at three different displacement rates varying from 0.005 mm/min to 0.1 mm/min by varying the size of the specimen. While small soil specimens exhibited increased shear strength when the loading displacement rate was increased, medium and large-sized soil specimens showed a decrease in shear strength as the loading displacement rate was decreased. Luo *et al.* (2025) investigated the mechanical behavior of artificially stratified soils composed of silty clay and silty sand layers. This layered soil system was inspired by deposits from the Yangtze River floodplain in China. The artificial layered soil samples were prepared ensuring uniform layering and repeatability. The prepared soil samples were subjected to consolidated-undrained triaxial tests under varying layer thicknesses, consolidation conditions, and loading paths. The results show that the behavior of layered soils lies between that of pure silty clay

and silty sand, with thicker clay layers shifting behavior toward a clay-like response and thinner ones toward a sand-like response. Importantly, the laminated soil structure enhances volumetric dilation, increases undrained shear strength, and suppresses shear band development. This research emphasized that preserving natural layering in soil systems is crucial, as disturbed samples may underestimate stratified soil strength and undermine the accuracy of geotechnical characterization in the design of related structures. Several other researchers have made use of UCS tests to estimate the unconfined compression strength of lateritic and stabilized expansive soils (Ali *et al.* 2020, Wang *et al.* 2020), assess the mechanical properties of dredged soil from coal mine stabilized with cement and lime (Chompoorat *et al.* 2021), to characterize the strength of black cotton soil stabilized by bagasse ash-lime mixture (Ramesh *et al.* 2022), to assess the influence of wood pellet on Korean weathered granite soil (Balagosa *et al.* 2024), to investigate the strength of cement-treated expansive organic subgrade soil (Sagidullina *et al.* 2024), to determine the strength of lime- and cement-stabilized soils through freeze-thaw tests (Chhun *et al.* 2020, Jin *et al.* 2020, Jummasultan *et al.* 2021, Ibdah *et al.* 2025) as well as by the usage of chemical admixtures (Fard *et al.* 2020). In all the above-discussed studies, it can be observed that the tests are more focused on homogeneous soil samples. However, in laminated soil structures, layering can influence the strength characteristics and failure patterns. In addition to the varying number of layers in the soil, there are hardly any studies that determine the effect on shear strength with different combinations of water content and loading rate.

In addition to UCS tests on soils, studies have also examined shear strength characteristics at the contact surface with geosynthetics under varying strain rates. For instance, Safa *et al.* (2019) studied the interaction between clay and geogrid on the contact surface at different strain rates, varying from 0.75 to 2.25 mm/min, using a large-box direct shear test modified for a pull-out test. The obtained stress-strain graph exhibited a hardening interaction behavior between clay and geogrid. Furthermore, geogrid strength activation increased with higher vertical stress, while shear strength at the contact surface varied inversely with the strain rate. Another approach to considering strain rate variation is through numerical modeling. Mukherjee and Pathak (2023) investigated the rate-dependent mechanical behavior of Toyoura sand by varying its initial density and testing it at different confining pressures and strain rates (ranging from 5×10^{-5} /s to 5×10^{-1} /s). The model parameters used existing experimental data from drained triaxial tests on Toyoura sand. A MATLAB code was developed with a fully explicit stress update algorithm to perform drained triaxial simulations. A 60% increase in peak shear strength was observed over four orders of magnitude in strain rate, indicating that strength increased with increasing strain rate. Additionally, the peak friction angle increased by 15–20% as strain rate increased, particularly in dense sand. In dense sand, the strain at peak increased with higher strain rates (delayed peak), whereas in loose/medium sand, the strain at peak decreased with higher strain rates (early peak). Several researchers,

including Wang and Cong (2019), Martinez and Stutz (2019), Zhang *et al.* (2022), Gruchot and Zydroń (2024), and Liu *et al.* (2024) have conducted tests to determine shear strength variation by varying the displacement rate using small direct shear tests, ring shear test apparatus, and triaxial tests. The triaxial test is very difficult to conduct on large sample sizes, such as in the present study, especially if the soil involved has significant clay content. In the case of other tests, such as direct shear and ring shear tests, the shearing is applied in a horizontal direction, unlike in UCS tests where samples are tested by loading them axially. Also, it is not possible to conduct direct shear and ring shear tests with as many laminae as used in this study, given the small size of the samples that can be tested on these devices. Therefore, the use of UCS tests in the present study to examine the shear strength of soil profiles and their failure patterns under different combinations of various numbers of layers, moisture contents, and loading rates is suitable, given the large number of samples to be tested.

While several of the above-discussed studies have advanced understanding of either homogeneous soils, rate-dependent strength behavior, or layered soils to some extent, these studies rarely provide an integrated evaluation of how moisture content, displacement rate, and variation in lamina thickness affect the strength and deformation in varved clays. More recent works on layered clays, such as those discussed above (e.g., studies by Zarei *et al.* 2023, Tornborg *et al.* 2023, Luo *et al.* 2025), highlight the importance of considering anisotropy and displacement rate effects in the study of soil strength but do not systematically combine these parameters under controlled laboratory conditions. The present study thus advances beyond existing works by systematically varying and combining different variables, namely the number of laminae, moisture contents, and loading displacement rates, in reconstituted varved clay samples and directly comparing their behavior with homogeneous counterparts. This approach provides mechanistic insights into how lamina interactions and soil fabric govern undrained shear strength and failure modes with changes in moisture conditions and loading displacement rate, representing a novel contribution that has not been explicitly addressed in earlier research.

Given the increasing construction in permafrost regions over the past few decades, understanding the strength properties of glacial soils has become crucial (Du *et al.* 2016). Glacial override, the process of glaciers moving over existing soils, influences its strength, deformation, and stability. This behavior is further complicated by moisture content variations during the glacial overriding. This study addresses these aspects by conducting UCS tests on six different soil samples, which include homogeneous and reconstituted varved clay samples prepared at five moisture contents. Red Soil (RS) and Black Soil (BS) were selected based on laboratory geotechnical characterization to represent the laminae in actual varved clays. Two homogeneous soil samples are composed separately of RS and BS, while for the reconstituted varved clays, RS and BS are alternated in a repeating pattern to form four different samples with 2, 4, 8, and 16 layers. The five moisture contents at which these samples are prepared include the

moisture content corresponding to Optimum Moisture Content (OMC), two on the drier side of OMC (0.8 OMC and 0.9 OMC), and two on the wetter side of OMC (1.1 OMC and 1.2 OMC). To simulate glacial override, UCS tests in this study are conducted at three displacement rates of 1.25 mm/min, 0.24 mm/min, and 0.024 mm/min. The behavior of soils under different displacement rates provides a simplified simulation of how soils with varying compositions might respond to different loading rates, which, in this study, is considered analogous to the varying velocities of glacial movement on the soil. Although the absolute magnitudes of displacement rates used in the present study might be different from the actual glacial override velocities, the general trends observed through the study regarding the undrained shear strength of the soil and its failure patterns provide insights into the way in which the soil may respond to glacial override. This study is particularly relevant to geotechnical engineering in terrains of cold regions that experienced glaciation in the past. These formerly glaciated soils (both homogeneous and laminated) often retain a complex stress history and anisotropy which arise from past glacial overrides on these soils. Such soils may exhibit pronounced rate-sensitive behavior, wherein the undrained shear strength of soils may vary significantly with shearing or loading rate, moisture conditions, and laminae thickness. Replicating these conditions in the laboratory through controlled variations in loading displacement rate, moisture content, and, in the case of reconstituted varved clay samples, additionally varying the number of laminations in a fixed standard height of soil sample, as done in the present study, provides valuable insight into the likely engineering mechanism of the soils under real-world current loading scenarios. Further, cold regions are known to be highly sensitive to climate change, and hence climate-related processes such as intensified freeze–thaw cycling, progressive permafrost thaw, and shifts in precipitation patterns can alter in-situ moisture regimes, which can thereby affect soil strength and deformation behavior over time. The findings from this study can directly support the design and maintenance of structures on these soils, such as stable slopes, durable transportation embankments, and robust retaining structures, in cold-region environments in the long term.

2. Materials and methodology

The two soils, RS and BS, used in the present study were obtained from the vicinity of the IIT Guwahati campus. Various preliminary geotechnical investigations were carried out to determine the suitability of these soils to replicate the soils that constitute the laminae of actual varved clays. These geotechnical investigations are discussed in Section 2.1, and the methods of testing and sample preparation are discussed in Section 2.2.

2.1 Material characterization of RS and BS used as constituent laminae

Fig. 1 shows the deposition sites of RS and BS. This figure also includes an image of the soils collected in a tray

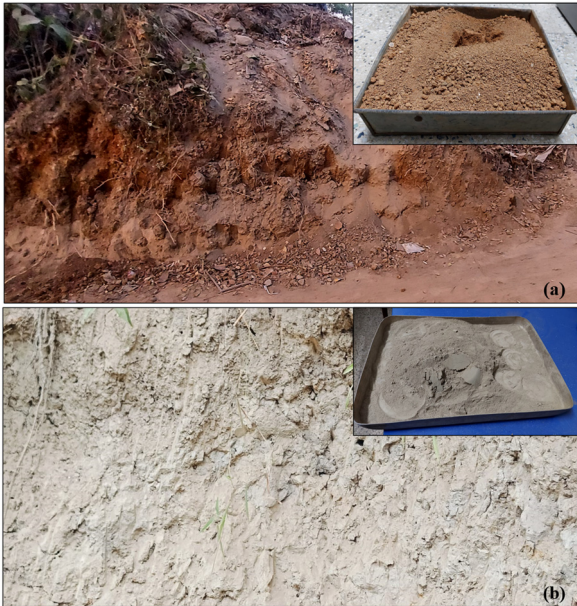


Fig. 1 Representative samples of (a) RS and (b) BS collected in the vicinity of IIT Guwahati campus

and dried. It can be observed that RS has a coarser texture, while BS has a finer texture. The preliminary geotechnical investigations conducted for selecting these soils include determining the Atterberg limits (IS: 2720 Part 5-1985) and Particle Size Distribution (PSD) (IS: 2720 Part 4-1980). These analyses revealed that RS can effectively represent the light-colored, silt-dominant laminae, while BS can represent the darker, clay-dominant laminae of actual varved clays. The laboratory tests, including these parameters of RS and BS along with other important geotechnical parameters that help in assessing their engineering behavior, are listed in Table 1.

From Table 1, it is observed that the liquid limits of RS and BS are 45% and 95%, respectively. The liquid limit is often associated with the clay content in soils, with soils that have higher clay content tending to have a higher liquid limit. This aligns well with the findings of the PSD, which show that BS has a significantly higher clay content of 84.9%, compared to RS, which has a lower clay content of 22.4%. The plastic limits of RS and BS are 19% and 30%, respectively. In comparison to RS, the higher plastic limit of BS indicates that it requires more moisture to make transition from a plastic to a semi-solid state. Practically, this means that BS has a greater ability to retain water while maintaining a plastic consistency. Additionally, the plasticity index of 26% for RS reflects its moderate plasticity, whereas BS demonstrates significantly higher plasticity with an index of 65%. The plasticity index values provide insight into the range of moisture over which each soil exhibits plastic behavior. In this case, BS exhibits plastic behavior over a wider range of moisture content compared to RS. From the grain size distribution, RS is found to have a composition of 23.2% sand, 54.4% silt, and 22.4% clay, while BS is characterized by 8.4% sand, 6.7% silt, and a predominant 84.9% clay content. These gradations in RS and BS have direct and competing implications for workability, packing density, and strength

Table 1 Geotechnical properties of RS and BS

Geotechnical Properties	Red Soil (RS)	Black Soil (BS)
Specific Gravity	2.7	2.6
Atterberg Limit (%)		
Liquid Limit	45	95
Plastic Limit	19	30
Plasticity Index	26	65
Compaction Characteristics		
Maximum Dry Density (g/cc)	1.77	1.59
Optimum Moisture Content (%)	19.5	21.5
Grain Size Distribution		
Sand	23.2	8.4
Silt	54.4	6.7
Clay	22.4	84.9
Soil Classification	ML	CH
Shear Strength Parameters		
Effective Friction Angle (°)	17.53	13.0
Cohesion (kPa)	12.4	6.1

development in prepared soil samples. The coarser matrix of RS has lower water retentive nature, as evident from its lower OMC of 19.5% (as compared to that of BS), and facilitates easier compaction to a higher MDD of 1.77 g/cc as compared to the MDD of BS. This dense, frictional packing contributes significantly to the higher shear strength of RS, as evidenced by its greater effective friction angle of 17.53° as compared to that of BS. Conversely, the high clay fraction of BS results in a higher specific surface area of the soil particles, which may lead to a high affinity for water and results in a higher OMC of 21.5%. This indicates that BS can have a significantly greater water demand during mixing to achieve workable consistency. Due to the fines in BS, it may have strong electro-chemical attractions and a water-retentive nature, which result in a lower MDD of 1.59 g/cc and dominate its undrained shearing behavior, leading to its lower shear strength.

These variations in grain size distribution and Atterberg limits contribute to the divergent engineering behavior of the soils when placed in layers to form the laminae of varved clays. The dominance of clay in BS and the higher silt content in RS are noteworthy and explain the differences in Atterberg limits. Furthermore, according to the classification system, RS is classified as ML (silt with low to medium plasticity), while BS is classified as CH (clay with high plasticity). These parameters of RS and BS are consistent with the characteristics of actual varved clays documented in the literature by Eden (1955), Kazi (1967), Eigenbrod and Burak (1991), Lydzba and Tankiewicz (2012), Florkiewicz *et al.* (2014), Tankiewicz (2016), Krawczyk and Szymanska (2018), and Flieger-Szymanska *et al.* (2019). Table 1 also lists other parameters obtained from laboratory tests, such as specific gravity (IS: 2720 Part 3/Sec-2-1980), compaction characteristics (IS: 2720 Part-7-1983), and shear strength parameters. The shear strength parameters were obtained from Direct Shear Tests (DST) conducted according to ASTM D3080/D3080M (ASTM 2012).

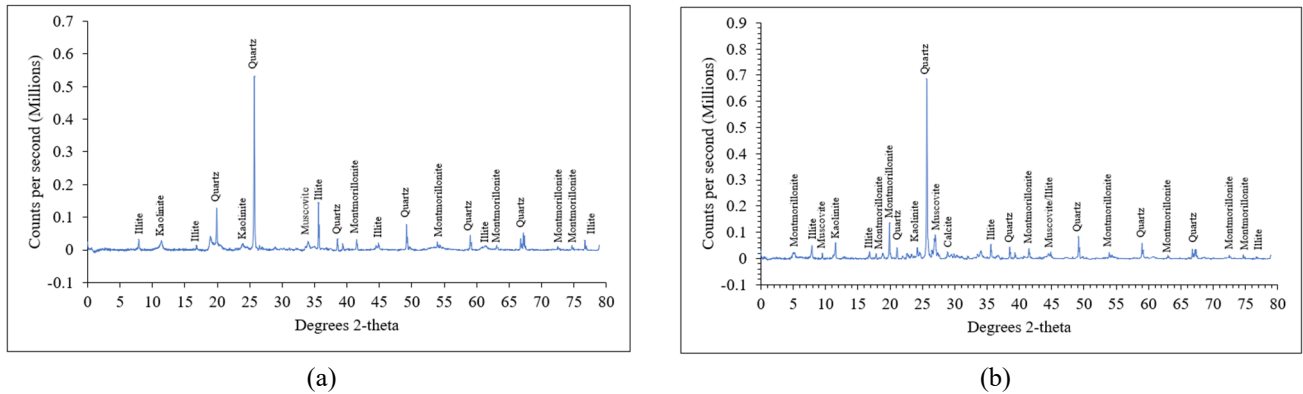


Fig. 2 X-ray Diffraction spectra of (a) RS (b) BS samples

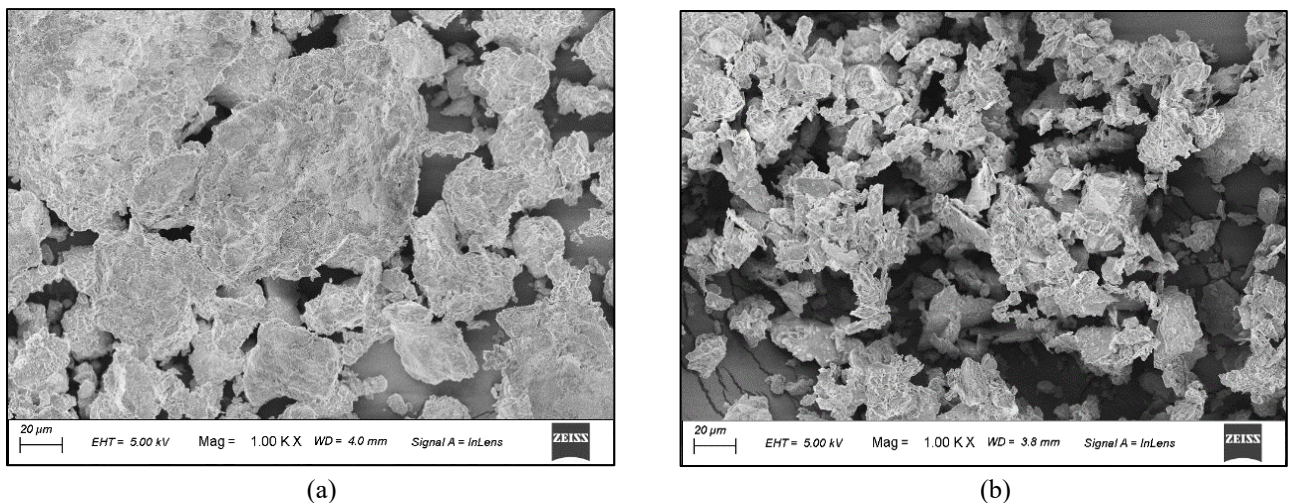


Fig. 3 Field Emission Scanning Electron Microscopy (FE-SEM) showing microstructure of (a) RS (b) BS at 1000X magnification

2.1.1 Mineralogical and morphological characteristics of RS and BS

To further ensure that RS and BS, used as representative soils in reconstituted varved clays, are mineralogically similar to the two laminae in actual varved clays, X-ray Diffraction (XRD) and Field Emission Scanning Electron Microscopy (FESEM) were conducted. Figs. 2(a) and 2(b) present the results of the XRD analysis, while Figs. 3(a) and 3(b) show the outcome of the FESEM analysis for RS and BS, respectively. The difference between these analyses is that the XRD technique examines the crystal structure of the soil, while the FESEM technique focuses on the microstructure of the soil. XRD works by illuminating the soil samples with X-ray beams and then measuring the angles and intensities of the beams scattered by the crystal lattice of the soil grains. On the other hand, in FESEM, electron beams are directed onto the sample with the help of electromagnetic lenses.

For conducting XRD analysis of RS and BS, the soils were finely ground and dried in the oven for 24 hours. The soils were then taken out of the oven, and the samples were placed on a glass sample holder. To ensure that the powdered sample didn't blow away and stayed in place, the soil was gently pressed with a glass slide. The excess soil

powder was removed with the same glass slide, and care was taken to ensure that the surface of the soil sample was smooth. This process was done separately for RS and BS. The prepared soil samples were then placed in a sample holder inside the XRD instrument, which consists of a detector. When the X-ray beams interact with the crystal lattice of the minerals in the soils, diffraction patterns are obtained. The X-ray diffraction patterns are produced by varying the angle at which X-rays strike the soil samples. The intensity of diffracted X-rays at different angles is used to create XRD patterns. The peak positions and intensities of the XRD patterns are compared with reference patterns available in literature or a database to identify the mineral composition in RS and BS, as shown in Figs. 2(a) and 2(b). A detailed interpretation of the XRD patterns from these figures confirms the primary mineral phases and highlights key differences between the mineralogical composition of RS and BS. The dominant phase in both soils is quartz, as indicated by the intense and sharp peaks at approximately 2θ values of 20.8° , 26.6° , and 50.1° , with the peak at 26.6° being the most intense in both XRD patterns of RS and BS. Kaolinite is clearly identified by its characteristic set of peaks at 2θ values of 12.4° , 24.9° , and 38.3° . Illite is indicated by its primary peaks at approximately 2θ values

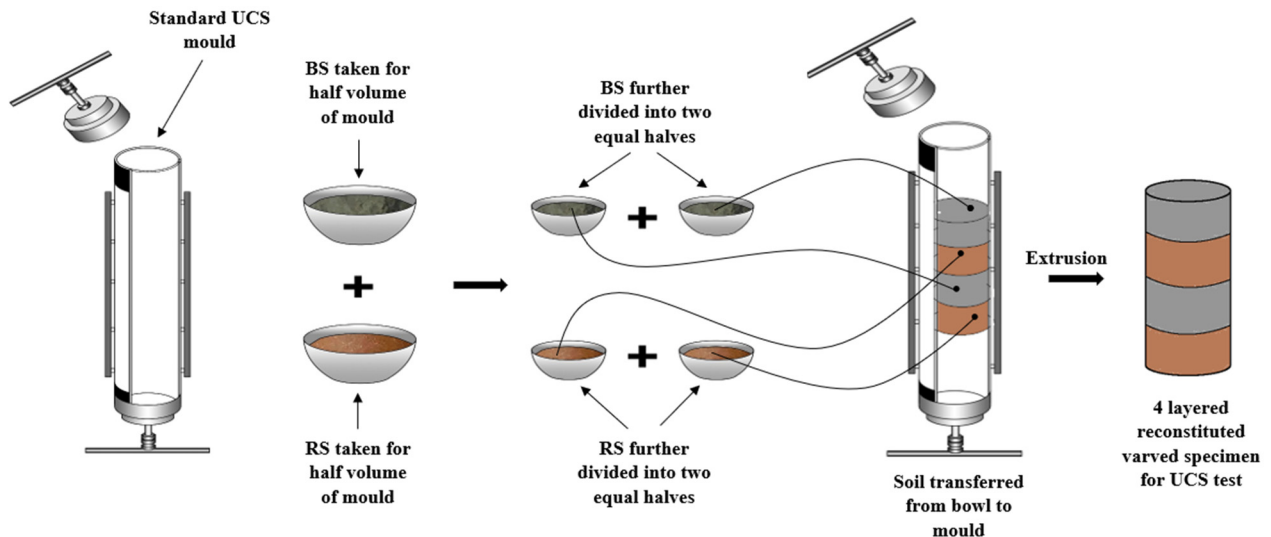


Fig. 4 Illustration of the sample preparation process for 4-layered reconstituted varved clays used in UCS testing

of 8.8° and 17.7° . The critical difference between the two spectra is the pronounced peak at approximately 2θ values of 5.8° and 18° – 20° in the BS sample, which shows the peak of montmorillonite and indicates its presence in BS. This peak is notably absent or very weak in the RS pattern, confirming a significantly higher montmorillonite content in BS. Thus, the XRD patterns clearly indicate that BS contains a significant amount of the clay mineral montmorillonite compared to RS. The higher proportion of swelling minerals like montmorillonite in BS is the fundamental reason for its expected higher plasticity, significant swelling potential upon hydration, and lower shear strength as compared to RS. A similar observation was reported by Ringberg and Erlström (1999). In this study, the researchers performed XRD by separating the summer layer (the lighter lamina) and the winter layer (the darker lamina) of varved clay. A significant difference was found between the XRD diffractograms of the two soils, particularly in the clay mineral peaks, with the winter layers showing higher magnitudes of these peaks. Blondeau (1975) also reported that when the dark and light laminae were X-rayed separately, they were found to be mineralogically identical, except for the higher clay content in the dark-colored laminae compared to the light-colored laminae. The author further reported the dominance of illite in the light-colored laminae with minor montmorillonite, whereas montmorillonite dominated the dark-colored laminae. This finding aligns with the XRD results of RS and BS obtained in the present study. This mineralogical difference between the soils RS and BS provides a direct mechanistic explanation for the anticipated geotechnical behaviors.

Fig. 3 displays the microstructure of RS and BS using FESEM analysis. FESEM analysis requires even more careful sample preparation than XRD. For FESEM, just like in XRD, both RS and BS were finely ground and oven-dried for 24 hours. Also, testing soils for FESEM is more difficult than conducting XRD analysis because, in FESEM analysis, the soil sample can absorb moisture from the

atmosphere during the sample preparation stage and can simultaneously develop electric charges on its surface. If this occurs, the images obtained through FESEM may not be clear, and many white patches can appear in the images. To avoid moisture exposure, both RS and BS samples were immediately transferred to an airtight box filled with silica beads after being removed from the oven. For the FESEM analysis, both samples were mounted on the same stub using sticky carbon tape. To prevent the buildup of charges on the surface of the soil sample due to moisture in the environment, once the samples were placed on the stub, they were coated with gold. The samples were then inserted into the FESEM machine, and images were captured at 1000X magnification, as this magnification provided the clearest images. From the captured images, it was observed that the particles of RS appeared larger and more rounded (Fig. 3(a)), while BS exhibited flaky-shaped particles (Fig. 3(b)). Clay particles are generally flaky in shape. Moreover, comparing the network of pores between the particles of both soils, higher porosity was observed in BS compared to RS. This can be attributed to the presence of clay minerals with a highly flocculated structure, leading to a larger number of inter-floc voids. Therefore, based on the mineralogical compositions and microstructure of the chosen RS and BS, it is concluded that the light-colored and dark-colored laminae of actual varves from glaciated regions can be suitably represented by RS and BS, respectively.

2.2 Methodology

All the soil samples for UCS testing are prepared by weighing the soil according to its Maximum Dry Density (MDD). The water content used for preparing these samples is based on the OMC. The five water contents selected for sample preparation are OMC, 1.2 OMC, 1.1 OMC, 0.9 OMC, and 0.8 OMC. The MDD and OMC were obtained by conducting the Standard Proctor Test (IS: 2720 Part-7-1983) on both soils. The MDD and OMC for RS are found

to be 1.77 Mg/m³ and 19.5%, respectively, while for BS, the corresponding values are 1.59 Mg/m³ and 21.5% (Table 1). The lower OMC of RS is attributed to the high presence of silt-sized particles, which allows better packing and helps in achieving MDD at a lower moisture content compared to BS. The higher OMC of BS is attributed to its high clay content, which requires a substantial amount of water for proper compaction.

The standard stainless-steel UCS mould, with a volume of 86,192.74 mm³, is used to prepare samples with a diameter of 38 mm and a length of 76 mm. The homogeneous soil samples are prepared by following routine sample preparation steps for UCS testing. First, the required weight of soil is calculated by multiplying the MDD of the soil with the volume of the standard mould used for preparing the sample for testing. The soil is then placed in a bowl and mixed with the designated moisture content. The mixture is transferred into the mould, and the mould is screwed from the ends. This standard mould is also illustrated in Fig. 4. Afterward, the sample is extruded using a sample extruding machine and immediately placed in the UCS machine for testing by positioning it between metal plates, without any curing period. The axial load is then applied to the sample at a constant chosen displacement rate of 1.25 mm/min, 0.24 mm/min, or 0.024 mm/min. The ends of all soil specimens were trimmed to be flat and perpendicular to the longitudinal axis to ensure uniform loading, and the diameter and height of each specimen were verified with calipers prior to testing.

For the reconstituted varved clay samples, the sample extrusion process remains the same, but the amount of RS and BS used varies. Since the proportion of RS and BS is consistent for the standard dimensions of UCS samples, regardless of the number of laminae in the reconstituted varved clay samples, the weight of each soil (RS and BS) also remains unchanged for all reconstituted varved clay samples. Fig. 4 illustrates the preparation of the 4-layered reconstituted varved clay sample used in the UCS test. To achieve this, half of the total volume of the mould is considered to calculate the weight of each soil type, with the appropriate amount of water added based on the desired moisture content relative to the OMC. In this example, the weights of RS and BS are measured to fill half of the volume of the mould, which is approximately 43,096.37 mm³ for each soil. The unit weights of RS and BS are 1.77 Mg/m³ and 1.59 Mg/m³, respectively (as shown in Table 1). Therefore, 76.28 g of RS and 68.52 g of BS are weighed separately into two containers, and the soil-water mixture is prepared. For the 4-layered reconstituted sample, these soils are further divided into two equal portions of 36.63 g of RS and 34.47 g of BS. The soils are then alternately transferred, layer by layer, into the UCS mould to form a 4-layered sample. Once the layers are placed, the mould is sealed with caps on both ends, and the sample is extruded for testing. This process is repeated for other varved clay samples, prepared at different water contents and with varying numbers of layers, following the same methodology.

For all the reconstituted varved clay samples, the soil samples are extruded and placed for UCS testing such that the lowermost lamina, which rests on the bottom plate,

always consists of RS. With the layers arranged alternately, the top layer is always BS, in contact with the top plate attached to the loading cell. The reconstituted varved clays are designated as 2L, 4L, 8L, and 16L in the study, where the numeric digits indicate the number of laminae, and 'L' stands for 'Laminae'.

To thoroughly analyze the influence of each variable, a full-factorial experimental design is adopted in the current study. This involves UCS testing of every combination of the three key parameters considered in the study, which include 6 soil profiles, 5 moisture contents, and 3 loading displacement rates. To assure statistical reliability and avoid any error, three identical specimens were prepared and tested for each unique combination. The undrained shear strength values presented in this paper are therefore the average of these three replicate tests. In total, this rigorous approach required the execution of 270 UCS tests, which form a comprehensive and reliable dataset for subsequent analysis.

3. Results and discussions

This section discusses the variation in undrained shear strength with respect to variables such as applied displacement rate and moisture content in both homogeneous and reconstituted varved clays, with additional consideration given to the varying number of laminae in the reconstituted samples. Additionally, different failure patterns under UCS loading for samples prepared and tested considering different combinations of these variables are also explored in this study. In Sections 3.1 and 3.2, the variation of undrained shear strength with respect to the chosen variables is discussed. Shear strength is an important property of soil that maintains equilibrium when the surface is uneven, such as in the case of slopes, or when loading on the soil induces shear stresses. In the UCS test, the applied axial stress generates shear stresses in the samples. The peak axial stress at which the soil sample fails is referred to as the unconfined compressive strength of the soil. According to the Mohr-Coulomb criterion, the unconfined compressive strength is related to the undrained shear strength, with undrained shear strength being half of the unconfined compressive strength. Since the study is conducted in the context of a glacial environment, where glacial override and hilly terrain prevail, the discussion focuses on the undrained shear strength across different soil profiles.

3.1 Variation of undrained shear strength with displacement rate and moisture content

Figs. 5(a)-5(f) show the variation of undrained shear strength with displacement rate for RS, BS, and reconstituted varved clay samples with 2, 4, 8, and 16 laminae, that are tested at different moisture contents. The general trend observed in all these graphs indicates that undrained shear strength decreases as the displacement rate increases for all soil profiles at different moisture contents. This demonstrates that when the axial loading rate on the

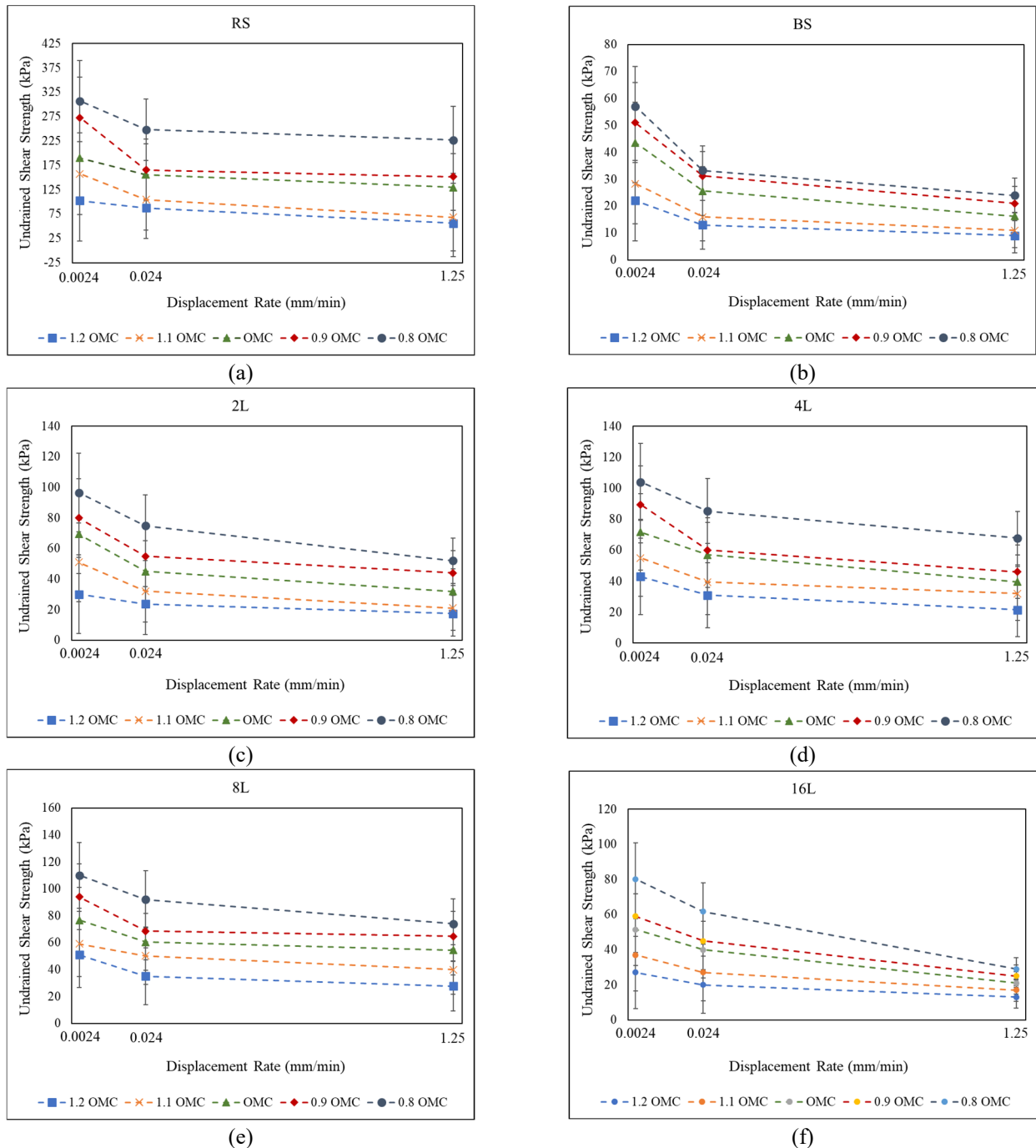


Fig. 5 Variation of undrained shear strength with displacement rate at different moisture contents for samples of (a) homogeneous RS soil, (b) homogeneous BS soil, and reconstituted varved clay samples with (c) 2L, (d) 4L, (e) 8L, and (f) 16L

soil decreases, its ability to resist shear stress increases. The increase in undrained shear strength of soils with the decrease in displacement rate is more pronounced when the rate lowers from 0.24 mm/min to 0.024 mm/min, compared to when it decreases from 1.25 mm/min to 0.24 mm/min. This non-linear behaviour suggests that soil samples exhibit greater sensitivity to undrained shear strength at lower displacement rates. This sensitivity occurs because slower displacement rates allow more time for the soil structure to mobilize its internal strength to resist loading. The

mobilization at low displacement rates occurs through the rearrangement and redistribution of internal stresses within the soil that result in increased undrained shear strength. In contrast, when the displacement rate is higher, soils exhibit more brittle behaviour with less opportunity for internal adjustment, which leads to failure at lower axial compressive loads. This suggests that in the actual field conditions, the rate of glacial movement governs the strength and stability of both layered and homogeneous soils. This behaviour is further supported by visual

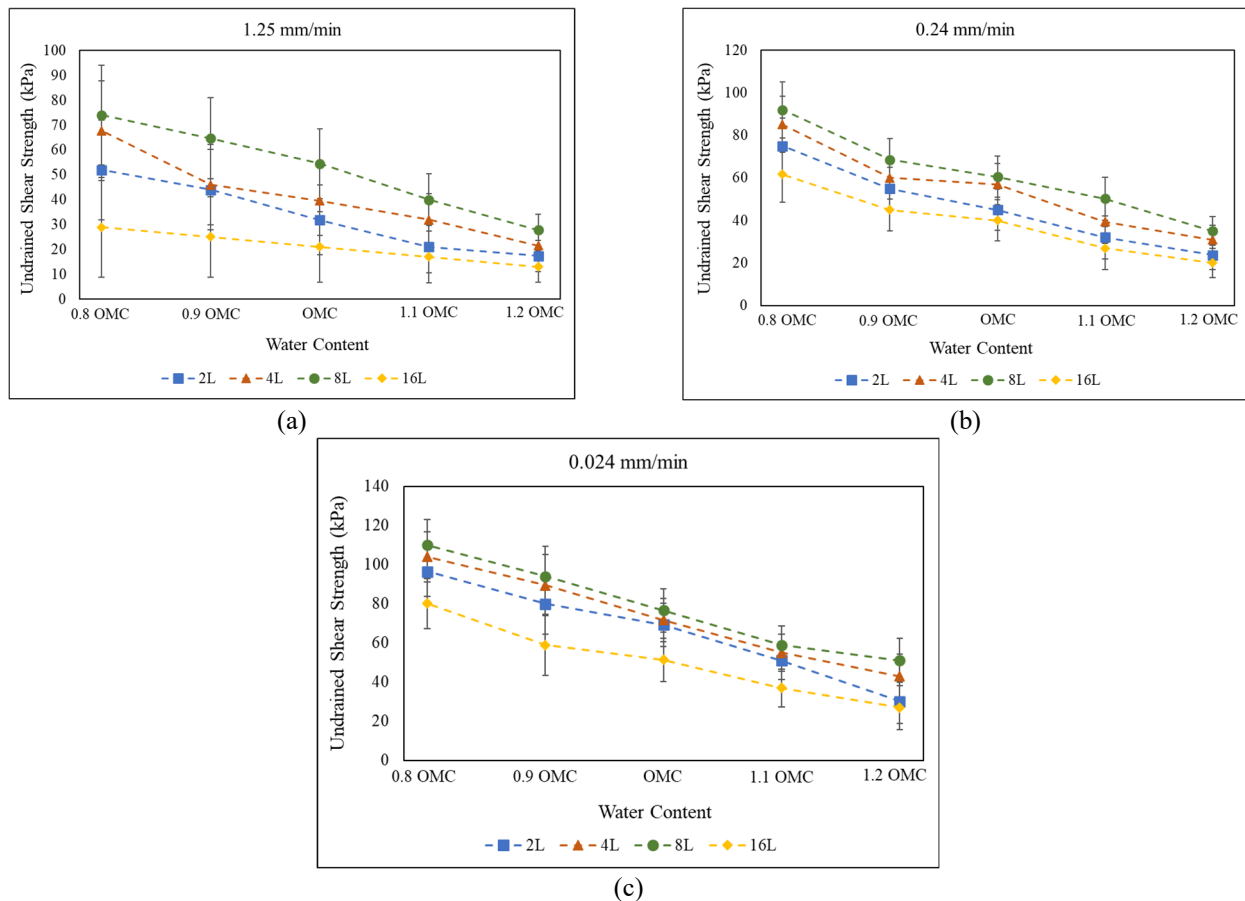


Fig. 6 Undrained shear strength variation with moisture content for reconstituted varved clay profiles with different lamina at displacement rates of (a) 1.25 mm/min, (b) 0.24 mm/min, and (c) 0.024 mm/min

observations of the failed soil samples after UCS testing shown in Figs. 9-14. These figures show that samples subjected to higher displacement rates experience shear-dominated, abrupt failure with sharp failure planes, indicating a brittle nature compared to those subjected to lower displacement rates. Since displacement rate is analogous to the velocity of glacial movement, it can be inferred that rapid glacial override on soils in cold regions leads to brittle, abrupt, and early failure of the underlying soils.

Additionally, it is observed that, among all the soil samples tested (Fig. 5), RS consistently exhibits the highest undrained shear strength (Fig. 5(a)), whereas homogeneous BS shows the lowest undrained shear strength (Fig. 5(b)). The reconstituted varved clay samples exhibit intermediate undrained shear strength, with values between those observed for homogeneous RS and BS. This pattern holds true for all combinations of displacement rates and moisture contents for the reconstituted varved clays. The higher undrained shear strength of RS is attributed to its higher shear strength parameters, i.e., the angle of internal friction and cohesion, compared to BS (Table 1). The high angle of internal friction allows for more compact packing of soil grains during sample preparation, while the high cohesion provides additional strength in the absence of lateral confinement, resulting in higher undrained shear strength for RS under unconfined axial loading compared to BS.

3.2 Variation of undrained shear strength with displacement rate, moisture content and number of laminae in reconstituted varved clays

Figs. 6 and 7 specifically focus on the variation in undrained shear strength for reconstituted varved clays with different moisture contents and numbers of laminae at a given displacement rate. The results from homogeneous RS and BS samples are not shown here, as the differences in undrained shear strength magnitudes between RS and BS would make the graphs difficult to interpret alongside the reconstituted varved clays. Moreover, the discussion on undrained shear strength for RS and BS has already been briefly covered in the previous section.

Fig. 6 shows the variation in undrained shear strength with moisture content for reconstituted varved clay profiles at different displacement rates of 1.25 mm/min (Fig. 6(a)), 0.24 mm/min (Fig. 6(b)), and 0.024 mm/min (Fig. 6(c)). From the graphs, it is observed that reducing the moisture content from OMC to 0.9 OMC and 0.8 OMC leads to an increase in undrained shear strength. Conversely, increasing the moisture content from OMC to 1.1 OMC and 1.2 OMC results in a decrease in undrained shear strength for all the soil profiles, irrespective of the applied displacement rates. However, the undrained shear strength values remain higher for samples tested at lower displacement rates, as discussed in Section 3.1. This decrease in undrained shear strength

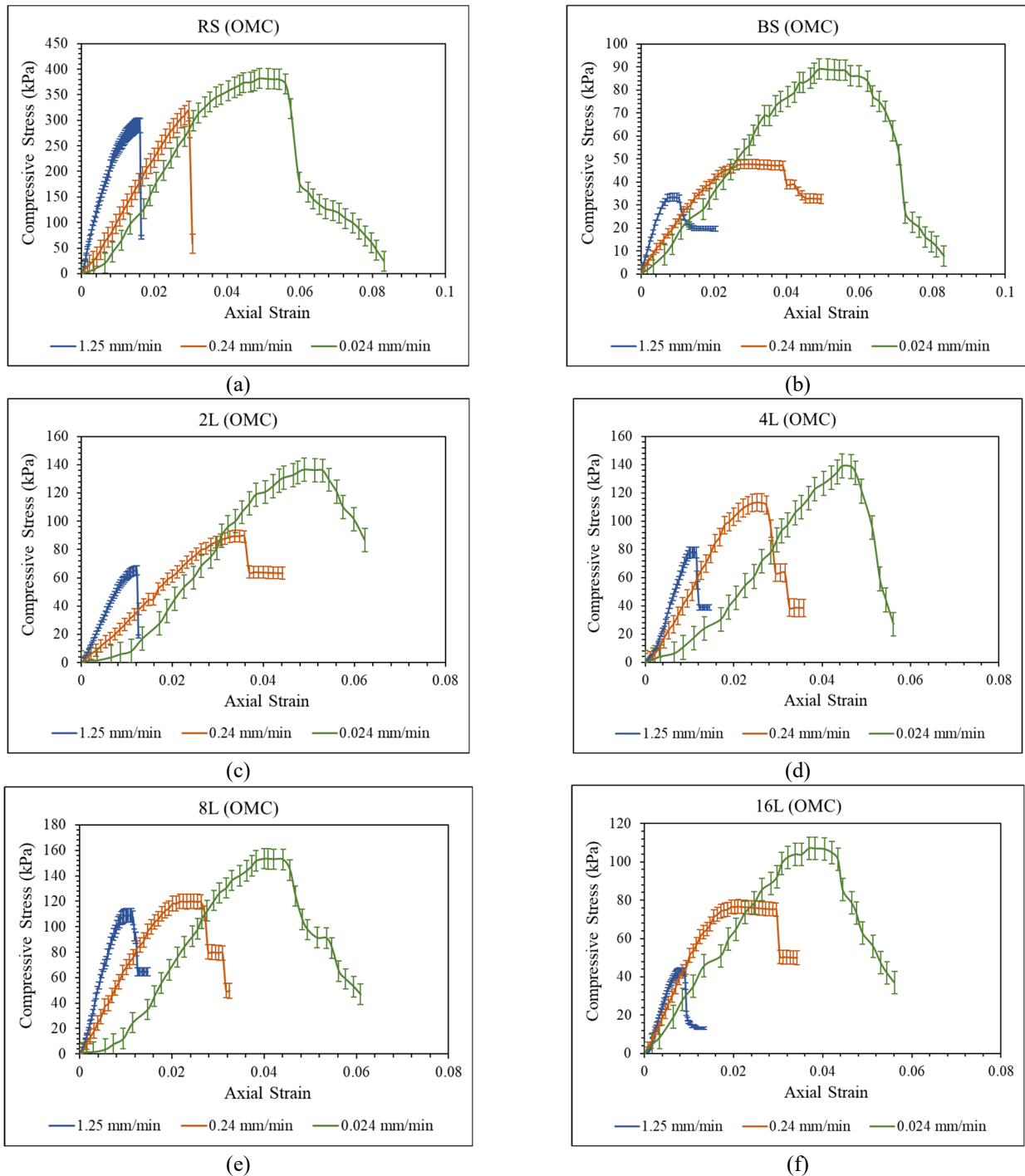


Fig. 7 Stress-strain curves under UCS loading at different displacement rates for samples prepared at OMC for (a) homogeneous RS, (b) homogeneous BS, and reconstituted varved clay with (c) 2L, (d) 4L, (e) 8L, and (f) 16L

with increasing moisture content occurs because excess water acts as a lubricant between soil grains, which reduces friction and cohesion between particles and makes the soil fail more easily under load. A decrease in moisture content, up to a certain limit, leads to greater frictional resistance between soil grains. At moisture contents of 0.9 OMC and 0.8 OMC, the undrained shear strength increases, which indicates that reduced moisture enhances interlocking between soil particles, leading to greater resistance to axial loading. The samples prepared at water contents lower than

OMC also become more rigid, which is observed in their failure patterns shown in Figs. 8-13. Also, for samples prepared at moisture content on the wetter side of OMC, significant challenges were encountered during the preparation phase. The samples frequently broke during the extrusion process due to their tendency to stick to the metal plates. Even after successful extrusion, the samples often became distorted while being placed between the two metal plates for UCS testing, making the samples prepared on the wet side of OMC difficult to handle. Due to these

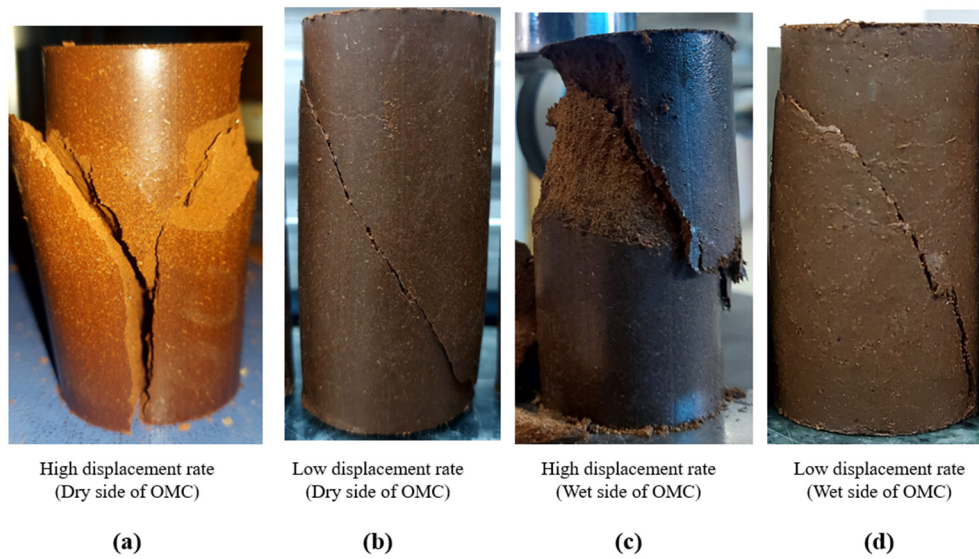


Fig. 8 Failed homogenous RS samples after UCS test under varying displacement rates and moisture content

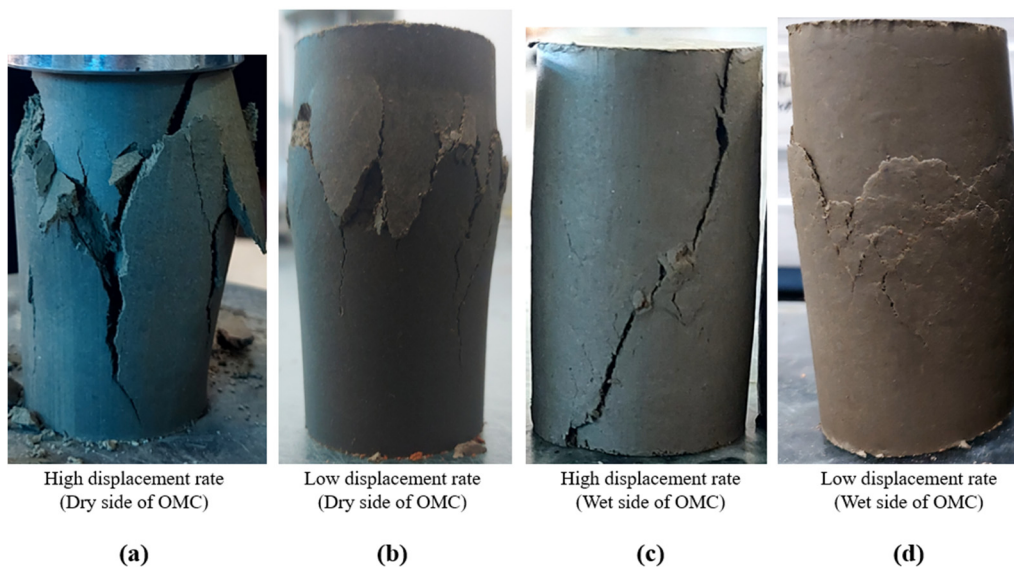


Fig. 9 Failed homogenous BS samples after UCS test under varying displacement rates and moisture content

challenges, careful handling was required for samples prepared at moisture contents above OMC. These observations and experiences during the preparation and handling of soil samples with high water content highlight the adverse effects of excess moisture on the strength and stability of the samples.

Another important observation from Figs. 6 is the asymmetry in the sensitivity of undrained shear strength to increases and decreases in moisture content relative to OMC. Notably, the decrease in undrained shear strength due to increase in moisture content (from OMC to 1.1 OMC and 1.2 OMC) is more pronounced than the increase in undrained shear strength for the same magnitude of moisture content decrease (from OMC to 0.9 OMC and 0.8 OMC) for all soil samples. For example, at a displacement rate of 1.25 mm/min for the 2L reconstituted varved clay sample, the undrained shear strength at OMC is 32 kPa.

When the moisture content is reduced to 0.9 OMC and 0.8 OMC for this sample, the undrained shear strength increases to 44 kPa and 52 kPa, respectively. However, when the moisture content is increased to 1.1 OMC and 1.2 OMC, the undrained shear strength decreases to 21 kPa and 17 kPa, respectively. The increase in undrained shear strength due to the reduction in moisture content from OMC to 0.9 OMC and 0.8 OMC is 1.38 times and 1.63 times the undrained shear strength at OMC, respectively. Conversely, the decrease in undrained shear strength due to the increase in moisture content from OMC to 1.1 OMC and 1.2 OMC is 1.52 times and 1.83 times the undrained shear strength at OMC, respectively. This asymmetry suggests that soils are more sensitive to increases in moisture content compared to equivalent decreases in moisture content relative to OMC. This difference in sensitivity is due to increased pore water pressure at higher moisture contents, which significantly

reduces the ability of soil to resist shear stresses, as discussed in Section 3.1. The higher pore water pressure lowers the effective stress within the soil, which weakens the bonds between particles and leading to earlier failure under axial loading.

From Fig. 6, it is evident that as the number of laminae in the reconstituted varved clay sample increases from 2 to 4 and then to 8, the undrained shear strength increases. However, when the number of laminae increases to 16, the undrained shear strength decreases significantly, with these values falling below those of the 2-layered reconstituted sample. The increase in undrained shear strength up to 8 layers suggests that adding laminae within a fixed length of soil enhances load resisting capacity up to a certain number of laminae. This improvement in strength is likely due to the interaction between RS and BS laminae, where the RS laminae act as reinforcement in the alternating arrangement with BS in the reconstituted varved clay profiles. This is evident from the fact that in homogeneous BS soil samples, where the entire sample consists of BS, the undrained shear strength is the lowest among all the soil profiles considered in this study at the given displacement rate and moisture content. However, when the same BS is alternated with RS to form a laminated structure, an increase in undrained shear strength is observed. The RS laminae in the reconstituted varved clays also provide a confinement effect, limiting the lateral expansion of the BS laminae when BS is sandwiched between RS laminae. This is particularly evident in the samples prepared at moisture contents above OMC, as shown in Figs. 10-12, which depict the failure patterns in the reconstituted varved clay profiles. Therefore, as the number of laminae increases in the reconstituted varved clays, the alternating arrangement of RS and BS enhances interlayer bonding and friction, contributing to increased undrained shear strength. However, when the number of layers reaches 16, a sharp decline in undrained shear strength occurs. This suggests that an excessive number of laminae introduces too many RS-BS interfaces within the soil samples, which now act as planes of weakness, reducing the overall strength during UCS testing. As a result, the RS laminae can no longer compensate for the weaker BS laminae, and the increased number of laminae outweighs the benefits of interlayer bonding between RS and BS, which leads to a decrease in strength. Additionally, the weakness of the 16-layered soil was evident during the sample extrusion process, as the layers often began to separate, particularly in samples prepared on the wetter side of OMC. At water content greater than OMC, these samples, among all other reconstituted varved clays, were more difficult to handle and place between the plates of the UCS machine, indicating mechanical instability caused by excessive layering and high-water content. From an engineering and modelling perspective, these findings related to the density of laminations in the varved clays highlight their non-linear strength behavior that cannot be captured by homogeneous soil assumptions. For design in varved clay regions, these observations imply that stratification density is a critical factor in the sense that while some layering may enhance the overall stability of the soil mass, excessive lamination

can reduce overall strength and increase brittleness. The present study therefore provides experimental insight that emphasizes the need to incorporate stratigraphic variability in layered soil models, such as in the case of varved clays, where layer arrangement and interface density should be explicitly incorporated into constitutive frameworks.

3.3 Stress-strain curves for different combinations of soil profile, displacement rate and moisture content

Fig. 7 presents the stress-strain curves for different types of soil samples prepared at the water content of OMC under the UCS test with the load applied at different displacement rates. From an initial observation, it is evident that in all the soil samples, the peak compressive stress is highest for the displacement rate of 0.024 mm/min, followed by 0.24 mm/min, with the lowest peak compressive stress observed for samples loaded at the displacement rate of 1.25 mm/min. The strains at which peak compressive stress is achieved are also highest for the soil sample loaded at the displacement rate of 0.024 mm/min, followed by 0.24 mm/min, and the lowest strain is observed for the displacement rate of 1.25 mm/min.

It is further observed that among all the six soil profiles and for all displacement rates, the homogeneous RS samples exhibit the highest peak strength (Fig. 7(a)), while homogeneous BS samples exhibit lower peak strength (Fig. 7(b)). However, the post-peak nature of the stress-strain curve for homogeneous RS indicates its brittle nature compared to BS at all applied displacement rates. The brittle behavior in homogeneous RS is particularly evident from its sharp stress-strain curve up to the peak stress at displacement rates of 1.25 mm/min and 0.24 mm/min. This is followed by a steep drop in the curve post-peak strength to very low magnitudes of compressive stress at these displacement rates. These characteristics of stress-strain curve for RS indicates a sharp fracture of the sample. As the displacement rate is reduced to 0.024 mm/min, RS exhibits a more gradual stress-strain curve with a higher peak strength attained at higher strain magnitude. In this case, the post-peak drop is less sharp and does not fall to as low magnitudes as seen in the previous two higher displacement rates. Therefore, as the displacement rate is lowers, failure in homogeneous RS transforms to a less brittle nature. Comparatively, the stress-strain curves for homogeneous BS exhibit a gentler slope when approaching the peak stress, with noticeable plastic deformation before failure. After reaching the peak, a gradual strain softening is observed.

The stress-strain curves for reconstituted varved clays with 2, 4, 8, and 16 layers are shown in Figs. 7(c), 7(d), 7(e), and 7(f), respectively. Among the reconstituted varved clay profiles, as the number of laminae increases, the peak stress is achieved earlier, i.e., at smaller strains for a given applied displacement rate. For instance, at a displacement rate of 1.25 mm/min, the peak stress is reached at strains of around 0.012 and 0.0102 for the 2L and 4L reconstituted varved profiles, while for the 8L and 16L samples, it is approximately 0.009. At a displacement rate of 0.24 mm/min, the peak stress is attained at strains of 0.04, 0.034,

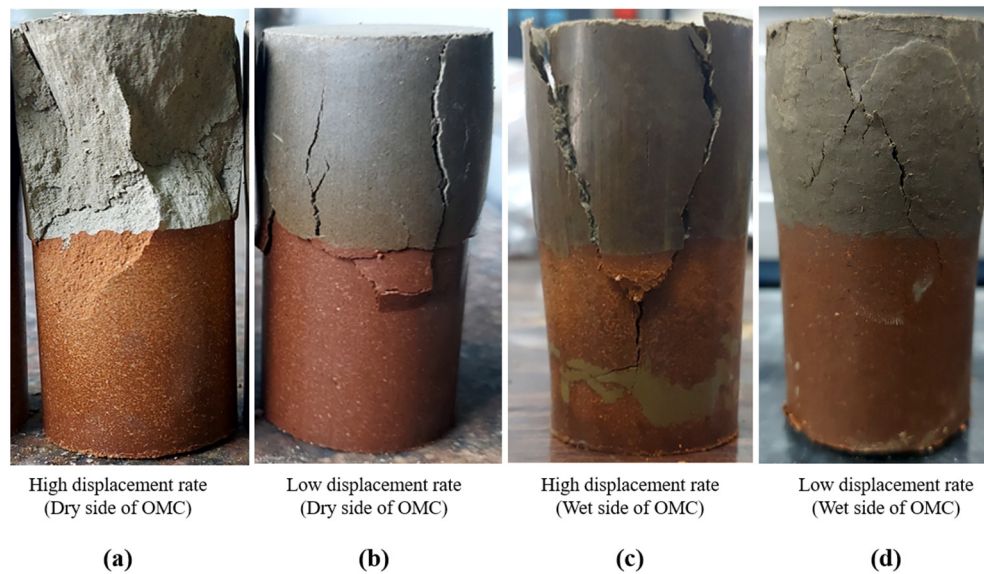


Fig. 10 Failed 2L reconstituted varved clay samples after UCS test under varying displacement rates and moisture content

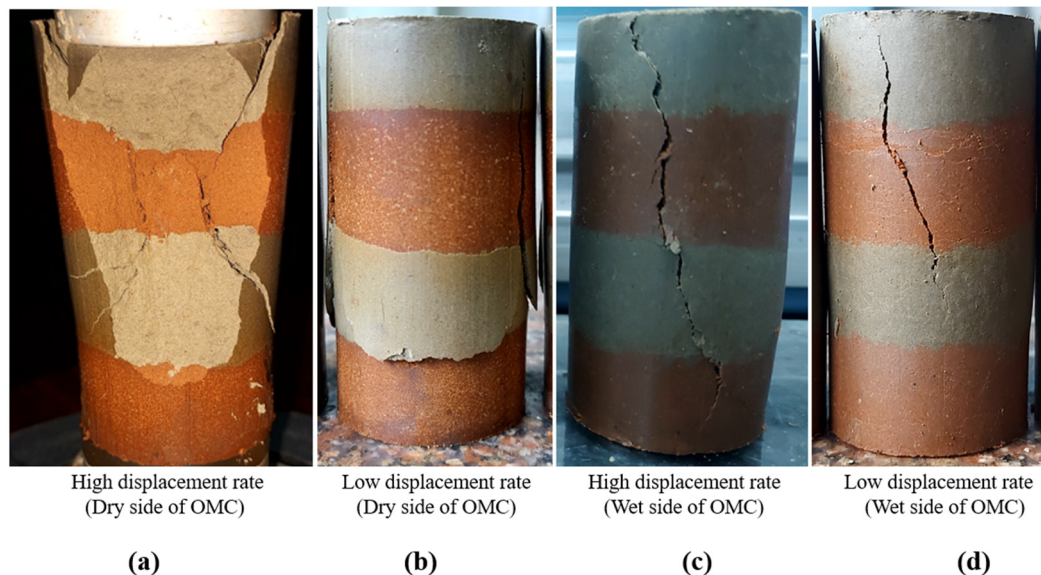


Fig. 11 Failed 4L reconstituted varved clay samples after UCS test under varying displacement rates and moisture content

0.026, 0.024, and 0.021 for the 2L, 4L, 8L, and 16L samples, respectively. For the displacement rate of 0.024 mm/min, the strain at which the maximum stress is reached is 0.049, 0.044, 0.04, and 0.036 for the 2L, 4L, 8L, and 16L samples, respectively.

From the stress-strain curve for samples loaded at a displacement rate of 0.24 mm/min, it is observed that as the number of laminae increases, the curve becomes flatter near the peak stress, indicating enhanced ductility in the samples as the number of laminae increases. However, for the other two displacement rates of 1.25 mm/min and 0.024 mm/min, the variation in the nature of failure with the increasing number of laminae, based on the stress-strain graph, is less clear.

These observations are specific to samples prepared at OMC. For conciseness, the stress-strain curves of samples prepared at other moisture contents are not shown here, as

the basic trend of the graphs remains the same. The only notable difference is that greater ductility is observed in the stress-strain curves for samples prepared at water content greater than OMC, with the peak compressive stress attained at slightly higher strain magnitudes for a sample loaded at given displacement rate. Conversely, samples prepared at lower moisture content than OMC become more brittle, achieving peak stress at lower strains.

3.4 Visual analysis of failed soil samples under UCS loading

Figs. 8-13 display the failure patterns of UCS-tested homogeneous RS (Fig. 8), BS (Fig. 9), and reconstituted varved clay samples consisting of 2L (Fig. 10), 4L (Fig. 11), 8L (Fig. 12), and 16L (Fig. 13). To simplify understanding and representation, the failure mode is

by visible surface peeling (Fig. 8(c)). Unlike the abrupt failure observed in RS samples prepared at moisture content on the dry side of OMC, Fig. 8(c) suggests that higher moisture content allows for some plastic deformation before failure under the same loading rate. When tested at a lower displacement rate, the homogeneous RS sample prepared at moisture content on the wet side of OMC exhibits a single, less pronounced oblique failure surface, along with noticeable bulging and horizontal minor cracks (Fig. 8(d)). This smoother shear surface with minor cracks indicates that higher moisture content combined with a slower displacement rate allows for more gradual deformation, leading to greater absorption of stresses and resulting in a more ductile failure behavior.

Fig. 9 shows the failure patterns for homogeneous BS samples tested for UCS. For samples prepared on the dry side of OMC and tested at high displacement rates, a combination of multiple fracturing and axial splitting is observed (Fig. 9(a)). This behavior is due to the substantial amount of clay in BS (Table 1), which acts as a brittle material under dry conditions. In contrast, when the same sample is loaded at lower displacement rates, multiple fractures are still visible but appear less sharp and are accompanied by minor vertical cracks (Fig. 9(b)). The contrast in failure patterns of homogeneous BS samples prepared in the same way but tested at different displacement rates is attributed to the gradual soil grain adjustment at slower displacement rates. For the homogeneous BS sample prepared on the wetter side of OMC and tested at a high displacement rate, a single oblique failure surface with a smooth inclined failure plane is observed, which is indicative of ductile-type failure behavior (Fig. 9(c)). For the same sample tested at low displacement rates, bulging in the middle portion of the sample along with irregular cracks is observed, which indicates progressive failure (Fig. 9(d)). Such observation in Fig. 9(d) is attributed to the higher clay content in BS, followed by the sample being prepared at higher moisture content and subjected to gradual loading. The visual observations of failure modes in BS highlight its high sensitivity to moisture content compared to RS. This is evident from the significant transition in the patterns of failed samples of homogeneous BS, which shift from brittle behavior at high displacement rates in dry samples to ductile behavior at low displacement rates in wetter samples. These differences in the observed patterns of failed homogeneous samples of RS and BS emphasize the role of moisture content and displacement rate in determining the failure mechanisms in soils.

For the 2L reconstituted varved clay samples (Fig. 10), the failed samples show that damage under UCS loading is primarily observed in the BS lamina, with the RS lamina hardly being affected. For the 2L sample prepared at a moisture content below OMC and tested at a high displacement rate, a sharp fracture is observed in the BS lamina, with the fracture being parallel to the direction of load application (Fig. 10(a)). The fracture in this case is abrupt and brittle, causing the failed portion of BS to break off instantly, followed by pulling away some of the surficial soil from the RS lamina. Additionally, a rough and tortuous

shear plane is also observed to form within the BS lamina. When the 2L sample prepared at the same water content is subjected to loading at a lower displacement rate, multiple vertical slips form within the BS lamina (Fig. 10(b)). Also, shear generation in this failed sample is evident at the interface between the layers, where the RS and BS laminae show separation along the interface plane, with some surface layers of RS peeling off. There is also slight bulging in the BS lamina in both Figs. 10(a) and 10(b), with the RS lamina remaining mostly intact in both cases. In the 2L samples prepared at a moisture content on the wet side of OMC and tested at a high displacement rate, a wedge-shaped failure mass develops in the BS lamina, which results in the development of an axial splitting plane in the RS lamina (Fig. 10(c)). This means that the formed wedge in the BS lamina generates tensile forces in the RS lamina. For the same sample tested under low displacement conditions, ductile deformation with visible bulging in the BS lamina, followed by development of diagonal cracks is observed (Fig. 10(d)). In this case, the RS lamina also shows development of smooth cracks.

From the failure patterns of the 4L varved clay samples, it is observed that the lowermost lamina, consisting of RS, remains the least affected, while the failure plane clearly passes through the remaining three laminae (Fig. 11). Compared to the 2L varved samples (Fig. 10), where failure primarily occurs in the BS lamina, in the case of the 4L varved samples subjected to UCS loading, although the lowermost lamina consisting of RS remains the least affected, the other RS lamina is affected during sample failure due to being sandwiched between low-strength BS laminae at both ends.

For the 4L reconstituted varved samples prepared at a moisture content below OMC and tested at a high displacement rate, a double shear failure resembling an X-shaped failure surface is observed (Fig. 11(a)). For the same sample tested at a low displacement rate, an axial split originates from the central lower portion of the sample in the BS lamina and extends upward into the RS laminae (Fig. 11(b)). For the same sample prepared at a moisture content on the wet side of OMC and tested at a high displacement rate, the formation of a smooth, gently inclined, tortuous shear plane along a single surface is observed, accompanied by slight bulging (Fig. 11(c)). When the same sample is tested at a low displacement rate, a smooth shear failure plane initiates from the uppermost BS-RS interface, which is indicated by significant horizontal cracking at this interface (Fig. 11(d)). The failure surface is vertical (perpendicular to the direction of layering) in the BS lamina and gently inclined in the sandwiched RS lamina. Slightly more bulging is observed in this case, particularly around the RS-BS interface in the middle portion of the sample. The gentle angle of failure plane ($< 45^\circ$) in Figs. 11(c) and 11(d) can be attributed the lamination in the soil profile.

In the failed 8L varved clay samples (Fig. 12), the failure patterns are observed to be more complex compared to the 2L and 4L varved samples. It is evident from the figure that the lowermost RS lamina remains relatively unaffected and intact, while the RS laminae sandwiched between BS laminae undergo shearing, similar to the 4L

varve case. For the sample prepared on the dry side of OMC and loaded at a high displacement rate, a tortuous "lambda"-shaped failure pattern is observed (Fig. 12(a)). The sharp and abrupt failure surfaces reflect the brittle nature of the failure. When the same sample is subjected to a lower displacement rate, the sample splits axially, and material breaks off from the middle portion, with vertical cracks forming around the failed sample (Fig. 12(b)). The upper portion appears plastically deformed, which indicates ductile nature of failure. For the sample prepared on the wet side of OMC and tested at a high displacement rate, multiple shearing planes develop with predominantly diagonal cracks and slight bulging (Fig. 12(c)). When the same sample is loaded at a lower displacement rate, vertical cracks with occasional diagonal cracks develop throughout the sample (Fig. 12(d)). The slight bulging, along with the gradual development of smooth cracks, indicates a greater degree of ductile deformation under slower loading conditions compared to the previous failed 8L varve sample in Fig. 11(c).

For the failed 16L varved clay samples prepared on the dry side of OMC and loaded at a high displacement rate, it is observed that the upper half of the sample forms a wedge, causing the lower portion to split axially (Fig. 13(a)). This is again a typical characteristic of brittle failure. For the same sample tested at a low displacement rate, a distorted Y-shaped failure surface is observed (Fig. 13(b)). The distortion is due to the presence of multiple laminae, while the smooth failure surface is attributed to the lower displacement rate. In the failed 16L varved samples prepared on the wet side of OMC and tested at high displacement rates, shear failure occurs along a single plane, passing through the entire height of the sample and affecting each lamina (Fig. 13(c)). For the same sample tested at a low displacement rate, multiple smooth vertical cracks are observed to develop, particularly through the middle portion of the sample (Fig. 13(d)). The crack development is smooth and progressive in nature.

Finally, it is observed that when samples are prepared on the wetter side of OMC, BS exhibits bulging under loading. Compared to the failure patterns of the laminated samples with 2L, 4L, and 8L varves, the least amount of bulging is observed in the 16L varved profiles. In fact, as the number of laminae increases, the bulging in the samples decreases. This suggests that as the number of layers increases and the thickness of the BS laminae decreases in the varved samples, the BS laminae, being sandwiched between RS laminae, experience restricted bulging.

3.5 Analysis of variance (ANOVA) for experimental data

To statistically assess the relative influence of soil type (homogeneous or varved clays with different numbers of laminae in fixed soil height), moisture content, and applied loading displacement rate on the undrained shear strength of soils, a two-way ANOVA without replication is performed in MS-Excel. Given that three independent factors have been varied in the current study (soil type, moisture content, and loading displacement rate), three sets of two-way

Table 2 Statistical significance of the effects of displacement rate and moisture content on undrained shear strength for different soil types

Soil Type	Effect of displacement rate	Effect of moisture content
RS	Extremely Significant ($F > F_c$, $p = 4.0 \times 10^{-4}$)	Extremely Significant ($F > F_c$, $p = 1.8 \times 10^{-5}$)
BS	Extremely Significant ($F > F_c$, $p = 7.3 \times 10^{-5}$)	Extremely Significant ($F > F_c$, $p = 7.5 \times 10^{-4}$)
2L	Extremely Significant ($F > F_c$, $p = 1.4 \times 10^{-4}$)	Extremely Significant ($F > F_c$, $p = 7.2 \times 10^{-5}$)
4L	Extremely Significant ($F > F_c$, $p = 3.3 \times 10^{-5}$)	Extremely Significant ($F > F_c$, $p = 9.4 \times 10^{-6}$)
8L	Extremely Significant ($F > F_c$, $p = 3.9 \times 10^{-5}$)	Extremely Significant ($F > F_c$, $p = 2.5 \times 10^{-6}$)
16L	Extremely Significant ($F > F_c$, $p = 6.7 \times 10^{-4}$)	Highly Significant ($F > F_c$, $p = 2.2 \times 10^{-3}$)

Table 3 Statistical significance of the effects of moisture content and soil type on undrained shear strength at different displacement rates

Displacement rate	Effect of moisture content	Effect of soil type
1.25 mm/min	Highly Significant ($F > F_c$, $p = 5.6 \times 10^{-3}$)	Extremely Significant ($F > F_c$, $p = 4.7 \times 10^{-6}$)
0.24 mm/min	Extremely Significant ($F > F_c$, $p = 1.4 \times 10^{-4}$)	Extremely Significant ($F > F_c$, $p = 2.3 \times 10^{-8}$)
0.024 mm/min	Extremely Significant ($F > F_c$, $p = 2.0 \times 10^{-4}$)	Extremely Significant ($F > F_c$, $p = 2.4 \times 10^{-8}$)

ANOVAs are conducted: (i) for a given loading displacement rate, the interaction between soil type and moisture content is evaluated, (ii) for a given soil type, the interaction between displacement rate and moisture content is evaluated, and (iii) for a given moisture content, the interaction between soil type and displacement rate is evaluated. The test is conducted at a 5% level of significance ($\alpha = 0.05$). For each analyzed variable, the F-value (F), F-critical value (F_c), and p -value are calculated, and the significance of the various variables considered in this study is determined by comparing F with F_c and checking whether p is smaller or greater than the adopted significance level, i.e., α (0.05).

In ANOVA, the F-value is a test statistic that compares the variance between group means to the variance within the groups. The F_c value is a threshold obtained from the F-distribution table based on the chosen significance level (i.e., 5%) and the degrees of freedom, which depend on the number of groups (between-group variation) and the number of samples within each group (within-group variation). $F > F_c$ suggests a stronger effect of the considered variable on the conducted test, while $F < F_c$ means that the considered variable in the study does not significantly influence the results or outcomes of the tests. The p -value represents the probability of observing the calculated F-value. A p -value less than the significance level (0.05 in this case) confirms the statistical significance of the variable considered in the study. The F-value by itself does not directly determine the statistical significance of the considered variables in the study. To assess the significance

Table 4 Statistical significance of the effects of displacement rate and soil type on undrained shear strength at different moisture contents

Moisture content	Effect of displacement rate	Effect of soil type
1.2 OMC	Extremely Significant ($F > F_c$, $p = 1.0 \times 10^{-3}$)	Extremely Significant ($F > F_c$, $p = 3.7 \times 10^{-6}$)
1.1 OMC	Highly Significant ($F > F_c$, $p = 7.2 \times 10^{-3}$)	Extremely Significant ($F > F_c$, $p = 1.5 \times 10^{-4}$)
OMC	Extremely Significant ($F > F_c$, $p = 2.6 \times 10^{-5}$)	Extremely Significant ($F > F_c$, $p = 8.7 \times 10^{-9}$)
0.9 OMC	Highly Significant ($F > F_c$, $p = 5.2 \times 10^{-3}$)	Extremely Significant ($F > F_c$, $p = 2.2 \times 10^{-5}$)
0.8 OMC	Extremely Significant ($F > F_c$, $p = 4.6 \times 10^{-5}$)	Extremely Significant ($F > F_c$, $p = 1.6 \times 10^{-9}$)

of a considered variable in the study, the calculated F-value is compared with the critical F-value from the F-distribution at a chosen significance level α . The p -value is then derived from the F-value, which provides a more direct criterion wherein the influence of a variable is considered statistically significant if the p -value is less than or equal to α , and not significant otherwise. Common conventions used in reporting include $p \leq 0.05$ as significant, $p \leq 0.01$ as highly significant, and $p \leq 0.001$ as extremely significant. The interpretation from the analysis is discussed with the help of Tables 2-4.

Table 2 presents the statistical significance of the effects of applied loading displacement rate and different moisture contents on the undrained shear strength of different types of soil specimens, including homogeneous soils (RS, BS) and reconstituted varved clays with varying numbers of laminae (2L, 4L, 8L, and 16L). The ANOVA results demonstrate that both the loading displacement rate and moisture content have statistically significant influences on the undrained shear strength of all the types of soil specimens considered in this study, as indicated by $F > F_c$ and $p < 0.05$. The effect of variation in loading displacement rate considered in the study is consistently extremely significant on the undrained shear strength of all the soil profiles. The effect of variation in moisture content on the undrained shear strength of different soil profiles is also consistently extremely significant in all cases, with the exception of the 16L profile, where it is highly significant.

Table 3 summarizes the statistical significance of the effects of moisture content and soil type (homogeneous and reconstituted varved clays with different numbers of laminations) on the undrained shear strength of soil at different applied loading displacement rates. The analysis reveals that both moisture content variation and soil type statistically significantly affect the undrained shear strength of soils across all the loading displacement rates. For the effect of moisture content on the undrained shear strength of soil, significance is observed at all displacement rates, with the strength of influence increasing as the loading displacement rate decreases. At the highest rate (1.25 mm/min), the effect is highly significant, whereas at intermediate and lower rates (0.24 mm/min and 0.024 mm/min), the effect is extremely significant. For the effect of soil type on the undrained shear strength of soil, the

influence is extremely significant at all displacement rates. The stronger significance of both variation in moisture content and soil type on the undrained shear strength of soil at lower loading displacement rates may be attributed to greater shear mobilization, greater mobilization of interfacial and fabric-controlled strength, and greater moisture redistribution, which may be attributed to the greater time availability under slower loading rates.

Table 4 presents the statistical significance of the effects of displacement rate and soil type on the undrained shear strength of soils at different moisture contents. The results indicate that both displacement rate and soil type significantly influence the undrained shear strength of soils across all moisture conditions, but the relative strength of their influence varies depending on the proximity to the OMC. For displacement rate, the effect on the undrained shear strength of soils is extremely significant at 1.2 OMC, OMC, and 0.8 OMC, while it is highly significant at 1.1 OMC and 0.9 OMC. For soil type, the effect on the undrained shear strength of soil is consistently extremely significant across all moisture levels. However, soil type has a consistently stronger influence on the undrained shear strength of soil than displacement rate across all moisture levels.

4. Conclusions

The present study investigates the behavior of two types of soil samples under UCS loading, which includes homogeneous and reconstituted varved clay. The samples are tested for combinations of variations in displacement rate and moisture content, with additional consideration of different number of laminae in reconstituted varved clay. The results demonstrate that these variables significantly affect the undrained shear strength of the tested soil samples. The key findings are summarized as follows:

- For all soil the profiles, the undrained shear strength consistently decreases with increasing displacement rate. This has been attributed to the limited internal stress redistribution when the soil is loaded at higher displacement rates, whereas at lower displacement rates, the soil structure has more time to mobilize internal strength which results in more more ductile behavior.
- The stress-strain graphs indicate that soil exhibits brittle behavior in samples prepared at moisture content lower than OMC and subjected to higher displacement rates, gradually shifting towards a more ductile state in samples prepared at higher moisture content than OMC and subjected to lower displacement rates. This is further supported by visual analysis of the failed samples. For instance, in samples prepared at low moisture content, those loaded at high displacement rates exhibit brittle, abrupt failure with sharp failure planes, while those loaded at lower displacement rates show gradual brittle failure with smoother failure planes. In contrast, for samples prepared at high moisture content, the difference between failures at varying displacement rates is more pronounced, with samples loaded at lower rates displaying progressive failure surfaces and slightly more bulging compared to those loaded at

higher rates. These observations suggest that both displacement rate and moisture content play key roles in determining the nature of failure in soils.

- The number of laminae in the reconstituted varved clay samples significantly influences the undrained shear strength and failure pattern of the soil. Increasing the number of laminae from 2 to 4 and then to 8 enhances the undrained shear strength. This increase is attributed to the confining effect of the RS laminae on the BS laminae, which results in stronger interlayer bonding. However, when the number of laminae reaches 16, the undrained shear strength decreases drastically, as the numerous interfaces act as planes of weakness. This suggests that there is an optimal number of laminae that maximizes the undrained shear strength, beyond which additional laminae become detrimental.
- Reducing the moisture content below the OMC in the soil samples leads to an increase in undrained shear strength, while increasing moisture content beyond OMC results in a sharp decline. This is due to the asymmetry in soil sensitivity to moisture variations, suggesting that soils are more sensitive to increases in moisture content than to decreases by the same amount, using OMC as the reference. This highlights the nonlinear relationship between soil strength and moisture content and demonstrates the critical role that moisture content plays in influencing the undrained shear strength of soils
- The statistical analysis confirms that displacement rate, moisture content, and soil type, all three variables, significantly influence the undrained shear strength of soils. Moisture content and displacement rate consistently show extremely significant effects on the undrained shear strength of the soil, with moisture influence being slightly less strong only in the 16L profile. Soil type (homogeneous and laminated soils with different numbers of layers) emerges as the most dominant factor, resulting in an extremely significant effect on the undrained shear strength of soil across all loading displacement rates and moisture levels. Overall, the findings highlight that soil type, whether homogeneous or stratified, moisture variation, and rate of loading conditions must be jointly considered to reliably assess undrained shear strength in soils.

Overall, the findings of this study highlight the complex interplay between displacement rate, moisture content, and laminae in determining the strength and failure behavior of both homogeneous and varved clay soils under unconfined axial loading. The displacement rate dependent strength reduction demonstrated in the study suggests that rapid loading conditions such as heavy construction traffic, blasting, or pile driving may trigger brittle failures with reduced capacity for bulging in varved clays, whereas slower, sustained loads may lead to progressive deformation with comparatively greater bulging. Also, bulging has been found to be more pronounced in varved clays with thicker laminae, which demonstrates the influence of micro-stratification of varved clays on deformation patterns of the overall soil profiles. Such laminae effects observed in the reconstituted varved clays of this study suggest that natural stratification in glacial deposits can either enhance or weaken stability depending on lamina thickness and

arrangement. Further, the strong sensitivity of strength to moisture variations highlights the importance of drainage control and the consideration of freezing and thawing cycles in cold regions, wherein even small increases in water content can sharply reduce the strength of the soil. Collectively, these findings emphasize that designs for slopes, embankments, and foundations in cold-region environments must explicitly consider displacement rate, moisture variation, and stratigraphy to ensure resilient and safe infrastructure performance in the long term. This work therefore provides valuable insights for understanding the engineering response of glacially deposited varved clays by underscoring the need for more detailed study of multi-layered soils to accurately capture their strength and deformation behaviors.

5. Limitations and future scope

While this study provides a comprehensive experimental dataset and comparison of the mechanical behavior of homogeneous soils and reconstituted varved clays with different laminae densities, certain limitations and opportunities for future work are acknowledged. The visual classification of failure patterns in the laminated specimens, while described in detail, has been conducted without the aid of a standardized framework for such complex laminated soil structures. Future research could employ advanced high-resolution imaging techniques to develop a quantitative and standardized classification system for failure modes in laminated soils. Furthermore, the present research on the experimental characterization of stress-strain behavior focuses on both homogeneous and laminated soil structures, and although the influence of key variables has been established, no attempt has been made to develop a constitutive model to mathematically represent the observed anisotropic, rate-dependent, and moisture-sensitive response. Future work can include the development of a model through a theoretical framework and numerical fitting of the obtained data, presenting an avenue to enhance predictive capabilities. Finally, the study is conducted on laboratory-scale specimens. The potential scale effects when transitioning these findings to field-scale applications, such as full-scale slopes or foundations, remain unexplored. Subsequent investigations could involve large-scale physical modeling or field testing to validate the findings and establish scaling relationships for the design of geotechnical structures in varved clay deposits.

Acknowledgments

This study belongs to a part of the project ‘Study of Glacial Dynamics and Sustainable Hydrological Resources in Arunachal Himalaya’ (Project No. DST/CCP/MRDP/185/2019(G) dated 13/03/2020). The project is supported by Department of Science & Technology (SPLICE – Climate Change Program), Ministry of Science and Technology, Govt. of India. The authors express their gratitude for receiving the financial support for the same.

References

- Ali, M., Aziz, M., Hamza, M. and Madni, M.F. (2020), "Engineering properties of expansive soil treated with polypropylene fibers", *Geomech. Eng.*, **22**(3), 227-236. <https://doi.org/10.12989/gae.2020.22.3.227>.
- ASTM D3080/D3080M (2011), *Standard test method for direct shear test of soils under consolidated drained conditions*, American Standard Testing Methods; West Conshohocken, PA: ASTM.
- Awolaye, O.A., Bouazza, A. and Rama-Rao, R. (1991), "Time effects on the unconfined compressive strength and sensitivity of a clay", *Eng. Geol.*, **31**(3-4), 345-351. [https://doi.org/10.1016/0013-7952\(1\)90016-E](https://doi.org/10.1016/0013-7952(1)90016-E).
- Balagosa, J.A., Lee, M.J., Choo, Y.W., Kim, H.S. and Kim, J.M. (2024), "Effect of wood pellet fly ash on strength and microstructure of Korean weathered granite soil", *Geomech. Eng.*, **38**(4), 335-352. <https://doi.org/10.12989/gae.2024.38.4.335>.
- Blondeau, K.M. (1975), "Sedimentation and stratigraphy of the Mount Rogers Formation, Virginia", MS Dissertation; Louisiana State University and Agricultural and Mechanical College. https://doi.org/10.31390/gradschool_disstheses.8236.
- Chompoorat, T., Likitlersuang, S., Sitthiwiruth, S., Komolvilas, V., Jamsawang, P. and Jongpradist, P. (2021), "Mechanical properties and microstructures of stabilised dredged expansive soil from coal mine", *Geomech. Eng.*, **25**(2), 143-157. <https://doi.org/10.12989/gae.2021.25.2.143>.
- Chhun, K.T., Choo, H., Kaothon, P. and Yune, C.Y. (2020), "Experimental study on the strength behavior of cement-stabilized sand with recovered carbon black", *Geomech. Eng.*, **23**(1), 31-38. <https://doi.org/10.12989/gae.2020.23.1.031>.
- Dobak, P., Kiełbasiński, K., Szczepański, T. and Zawrzykraj, P. (2018), "Verification of compressibility and consolidation parameters of varved clays from Radzymin (Central Poland) based on direct observations of settlements of road embankment", *Open Geosci.*, **10**(1), 911-924. <https://doi.org/10.1515/geo-2018-0072>.
- Du, H., Ma, W., Zhang, S., Zhou, Z. and Liu, E. (2016), "Strength properties of ice-rich frozen silty sands under uniaxial compression for a wide range of strain rates and moisture contents", *Cold Reg. Sci. Technol.*, **123**, 107-113. <https://doi.org/10.1016/j.coldregions.2015.11.017>.
- Eden, W.J. (1955), "A laboratory study of varved clay from Steep Rock Lake, Ontario", Report No. DBR-R-24, National Research Council of Canada - Division of Building Research. <https://doi.org/10.4224/20331506>
- Ehlers, J. (2022), "From Moulins to Glacial Valleys", In: *The Ice Age*. Springer, Berlin, Heidelberg. https://doi.org/10.1007/978-3-662-64590-1_5.
- Eigenbrod, K.D. and Burak, J.B. (1991), "Effective stress paths and pore-pressure responses during undrained shear along the bedding planes of varved Fort William Clay", *Can. Geotech. J.*, **28**(6), 804-811. <https://doi.org/10.1139/t91-097>.
- Fard, A.R., Moradi, G., Ghalehjough, B.K. and Abbasnejad, A. (2020), "Freezing-thawing resistance evaluation of sandy soil, improved by polyvinyl acetate and ethylene glycol monobutyl ether mixture", *Geomech. Eng.*, **23**(2), 179-187. <https://doi.org/10.12989/gae.2020.23.2.179>.
- Flieger-Szymanska, M., Machowiak, K., Krawczyk, D. and Wanatowski, D. (2019), "Characterisation of mineral composition and strength parameters of varved clays", *Proceedings of the 17th European Conference on Soil Mechanics and Geotechnical Engineering (ECSMGE 2019)*, Reykjavik, Iceland. <http://doi.org/10.32075/17ECSMGE-2019-0172>.
- Florkiewicz, A., Flieger-Szymanska, M., Machowiak, K. and Wanatowski, D. (2014), "Engineering properties of varved clays from the Junikowski Stream Valley in Poland", *Proceedings of the 4th International Conference on Geotechnical Engineering for Disaster Mitigation and Rehabilitation (4th GEDMAR)*, Kyoto, Japan.
- Girgis, N., Li, B., Akhtar, S. and Courcelles, B. (2020), "Experimental study of rate-dependent uniaxial compressive behaviors of two artificial frozen sandy clay soils", *Cold . Sci. Technol.*, **180**, 103166, 1-13. <https://doi.org/10.1016/j.coldregions.2020.103166>.
- Gruchot, A. and Zydroń, T. (2024), "Effect of shear rate and saturation on shear strength of mineral and anthropogenic soil", *Archiv. Civil Eng.*, **70**(2), 97-117. <http://doi.org/10.24425/ace.2024.149853>.
- Hampton, D. and Yoder, E.J. (1958), "The effect of rate of strain on soil strength", Joint Highway Research Project No. C-36-20B, Purdue University, Lafayette, Indiana, 116- 129.
- Hang, T. (2003), "A local clay-varve chronology and proglacial sedimentary environment in glacial Lake Peipsi, Eastern Estonia", *Boreas*, **32**(2), 416-426. <https://doi.org/10.1111/j.1502-3885.2003.tb01094.x>.
- Ibdah, L., Owusu, K., Behdad, A. and Eun, J. (2024), "Effects of freeze-thaw cycles on the unconfined compressive strength of lime- and cement-stabilized soils", *Geomech. Eng.*, **41**(1), 59-70. <https://doi.org/10.12989/gae.2025.41.1.059>.
- IS 2720 Part 3/Sec-2 (1980), *Methods of test for soils: Determination of specific gravity: Fine, medium, and coarse-grained soils*, Bureau of Indian Standards; New Delhi, India.
- IS 2720 Part 4 (1980), *Methods of test for soils: Grain size analysis*, Bureau of Indian Standards; New Delhi, India.
- IS 2720 Part 5 (1985), *Methods of test for soils: Determination of liquid limit and plastic limit*, Bureau of Indian Standards, New Delhi, India.
- IS 2720 Part 7 (1983), *Methods of test for soils: Determination of water content-dry density relation using light compaction*, Bureau of Indian Standards, New Delhi, India.
- Jin, H., Lee, J., Zhuang, L. and Ryu, B.H. (2020), "Laboratory investigation of unconfined compression behavior of ice and frozen soil mixtures", *Geomech. Eng.*, **22**(3), 219-226. <https://doi.org/10.12989/gae.2020.22.3.219>.
- Jummasultan, A., Sagidullina, N., Kim, J., Ku, T. and Moon, S.W. (2021), "Performance of cement-stabilized sand subjected to freeze-thaw cycles", *Geomech. Eng.*, **25**(1), 41-48. <https://doi.org/10.12989/gae.2021.25.1.041>.
- Kazi, A. (1967), "Aspects of the engineering geology of laminated glacial lake clays", Ph.D. Dissertation, Imperial College of Science, London.
- Krawczyk, D. and Flieger-Szymańska, M. (2018), "The value of plasticity index (IP) and liquidity index (IL) of North Polish ablation boulder clays and varved clays depending of the method of its determination", *Scientific Rev. Eng. Environ. Sci.*, **27**(2), 167-174. <http://doi.org/10.22630/PNIKS.2018.27.2.16>.
- Lacasse, S.M., Ladd, C.C. and Barsvary, A.K. (1977), "Undrained behavior of embankments on New Liskeard varved clay", *Can. Geotech. J.*, **14**(3), 367-388. <https://doi.org/10.1139/t77-041>.
- Lamoureux, S.F. and Bradley, R.S. (1996), "A late Holocene varved sediment record of environmental change from northern Ellesmere Island, Canada", *J. Paleolimnol.*, **16**, 239-255. <https://doi.org/10.1007/BF00176939>.
- Leroueil, S., Bouclin, G., Tavenas, F., Bergeron, L. and Rochelle, P.L. (1990), "Permeability anisotropy of natural clays as a function of strain", *Can. Geotech. J.*, **27**(5), 568-579. <https://doi.org/10.1139/t90-072>.
- Lindqvist, J.K. and Lee, D.E. (2009), "High-frequency paleoclimate signals from Foulden Maar, Waipiata Volcanic Field, southern New Zealand: An Early Miocene varved lacustrine diatomite deposit", *Sediment. Geol.*, **222**(1-2), 98-110.

- <https://doi.org/10.1016/j.sedgeo.2009.07.009>.
- Liu, S., Liao, C., Chen, J., Ye, G. and Xia, X. (2024), "Shear rate effect on clay-structure interface strength properties in various interface boundary conditions", *Soil Dyn. Earthq. Eng.*, **177**, 1-14. <https://doi.org/10.1016/j.soildyn.2023.108389>.
- Lo, K.Y. and Milligan, V. (1967), "Shear strength properties of two stratified clays", *J. Soil Mech. Found. Div. ASCE*, **93**(1). <https://doi.org/10.1061/JSFEAQ.0000928>.
- Luo, L., Yang, Y., Shen, Z., Zhang, W., Wang, Z., Wang, X., Gao, H. and Xu, Q. (2025), "Experimental study on the mechanical behavior of artificially prepared stratified soil in triaxial compression tests", *Acta Geotechnica*, **20**, 543-562. <https://doi.org/10.1007/s11440-024-02426-5>.
- Lydzba D. and Tankiewicz M. (2012), "Preliminary study of failure anisotropy characterization of varved clay", *AGH J. Min. Geoeng.*, **36**(2), 229-234.
- Martinez, A. and Stutz, H.H. (2019), "Rate effects on the interface shear behaviour of normally and overconsolidated clay", *Géotechnique*, **69**(9), 801-815. <https://doi.org/10.1680/jgeot.17.P.311>.
- Mousavi, F., Abdi, E., Ghalandarayeshi, S. and Page-Dumroese, D.S. (2021), "Modeling unconfined compressive strength of fine-grained soils: Application of pocket penetrometer for predicting soil strength", *CATENA*, **196**, 1-7. <https://doi.org/10.1016/j.catena.2020.104890>.
- Mukherjee, M. and Pathak, S. (2023), "Rate-dependent shearing response of Toyoura sand addressing influence of initial density and confinement: A visco-plastic constitutive approach", *Geomech. Eng.*, **34**(2), 197-208. <http://doi.org/10.12989/gae.2023.34.2.197>.
- Philippe, E.G.H., St-Onge G., Valet J.P., Godbout P.M., Egli R., Francus P. and Roy M. (2023), "Influence of seasonal post-depositional processes on the remanent magnetization in varved sediments from glacial lake Ojibway (Canada)", *Geochem. Geophys. Geosyst.*, **24**(3), 1-20. <https://doi.org/10.1029/2022GC010707>.
- Ramesh, H.N., Kulkarni, M.G.R., Raghunandan, M.V. and Nethravathi, S. (2022), "Mechanical and microstructural investigations on cement-treated expansive organic subgrade soil", *Geomech. Eng.*, **38**(4), 353-366. <https://doi.org/10.12989/gae.2024.38.4.353>.
- Ringberg, B. and Erlström, M. (1999), "Micromorphology and petrography of Late Weichselian glaciolacustrine varves in southeastern Sweden", *Catena*, **35**(2-4), 147-177. [https://doi.org/10.1016/S0341-8162\(98\)00098-8](https://doi.org/10.1016/S0341-8162(98)00098-8).
- Sabatini, P.J., Bachus, R.C., Mayne, P.W., Schneider, J.A. and Zettler, T.E. (2002), "Evaluation of soil and rock properties", Geotechnical Engineering Circular No. 5, Technical Manual. <https://rosap.nrl.bts.gov/view/dot/40554>.
- Safa, M., Maleka, A., Arjomand, M.A., Khorami, M. and Shariati, M. (2019), "Strain rate effects on soil-geosynthetic interaction in fine-grained soil", *Geomech. Eng.*, **19**(6), 533-542. <http://doi.org/10.12989/GAE.2019.19.6.533>
- Sagidullina, N., Kim, J., Satyanaga, A., Ku, T. and Moon, S.W. (2024), "Mechanical and microstructural investigations on cement-treated expansive organic subgrade soil", *Geomech. Eng.*, **38**(4), 353-366. <https://doi.org/10.12989/gae.2024.38.4.353>.
- Sahlabadi, S.H., Bayat, M., Mousivand, M. and Saadat, M. (2021), "Freeze-thaw durability of cement-stabilized soil reinforced with polypropylene/Basalt fibers", *J. Mater. in Civil Eng.*, **33**(9), 04021232. [http://doi.org/10.1061/\(ASCE\)](http://doi.org/10.1061/(ASCE)).
- Schneider, M.A., Whittle, R.W. and Springman, S.M. (2022), "Measuring strength and consolidation properties in lacustrine clay using piezocone and self-boring pressuremeter tests", *Can. Geotech. J.*, **59**(12), 2135-2150. <https://doi.org/10.1139/cgj-2021-0486>.
- Tankiewicz, M. (2015), "Experimental investigation of strength anisotropy of varved clay", *Procedia Earth and Planetary Sci.*, **15**, 732-737. <https://doi.org/10.1016/j.proeps.2015.08.116>.
- Tankiewicz, M. (2016), "Structure investigations of layered soil – varved clay", *Annals of Warsaw University of Life Sciences - SGGW Land Reclamation*, **48**(4), 365-375. <http://doi.org/10.1515/sggw-2016-0028>.
- Tornborg, J., Karlsson, M. and Karstunen, M. (2023), "Permanent sheet pile wall in soft sensitive clay", *J. Geotech. Geoenviron. Eng.* - *ASCE*, **149**(6). <https://doi.org/10.1061/JGGEFK.GTENG-10955>.
- Tyagi, A., Wong, Y.C.D. and Lee, F.H. (2019), "Effect of loading strain-rates on peak strength and drainage behaviour of cement-treated soils", *Proceedings of the 16th Asian Regional Conference on Soil Mechanics and Geotechnical Engineering*.
- Wang, Y. and Cong, L. (2019), "Effects of water content and shearing rate on residual shear stress", *Arabian J. Geosci.*, **44**, 8915-8929. <https://doi.org/10.1007/s13369-019-03922-7>.
- Wang, C.C., Lin, H.D., Li, A.J. and Ting, K.E. (2020), "Assessment of the unconfined compression strength of unsaturated lateritic soil using the UPV", *Geomech. Eng.*, **23**(4), 339-349. <https://doi.org/10.12989/gae.2020.23.4.339>.
- Zarei, C., Soltani-Jigheh, H. and Liu, Y. (2023), "Effects of strain rate and specimen size on the behavior of fine-grained soils", *Arabian J. Geosci.*, **16**, 244. <https://doi.org/10.1007/s12517-023-11344-x>
- Zhang, C., Li, D., Luo, C., Wang, Z. and Chen, G. (2022), "Research on creep characteristics and the model of artificial frozen soil", *Adv. Mater. Sci. Eng.*, **1**, 1-15. <https://doi.org/10.1155/2022/2891673>.

IC